CDF/ANAL/BOTTOM/CDFR/10756
Version 1.0
March 22, 2012

# dE/dx for pions, kaons and protons for 9 fb$^{-1}$ analyses

M.J. Morello
*INFN and University of Pisa*
F. Ruffini
*INFN and University of Siena*

**Abstract**

This note describes an accurate study of the $dE/dx$ response for charged pions, kaons and protons with momentum larger 2 GeV/$c$ for analyses with 9 fb$^{-1}$ (up to P38) of data collected. Huge samples of $D^{\star+}$-tagged $D^0 \to K^-\pi^+$ decays and $\Lambda \to p\pi^-$ decays have been used to provide universal curves for charged pions, kaons and protons. Templates of observed residual, intrinsic residual and correlation are provided for all these particles.

## 1 Introduction

Hadron identification is difficult at CDF II, since the detector was mostly designed for high-$p_{\rm T}$ physics measurements. For charged particles with $p_{\rm T} \geq 2$ GeV/$c$, a reasonably effective separation can be obtained from the rate of energy loss through ionization ($dE/dx$) in the gas that fills the active volume of the drift chamber.

The individual charge collections output by the COT are subject to several corrections (*hit-level* corrections), applied in the off-line production, to remove a number of detector related conditions: hit merging, electronic pedestal subtraction, path-length correction high-voltage correction, $z$ correction, angle and drift distance corrections, wire correction, super-layer correction, and pressure correction. An exhaustive description of these corrections can be found in Ref. [1]. In addition to the hit-level corrections an accurate calibration of the uniformity of the $dE/dx$ response in time and over the chamber volume is required, see Ref. [2]. This is determined using track-oriented parameters ($\varphi_0$, $\eta$, hit multiplicity, time, secance, instantaneous luminosity) which allow complementary corrections accounting for some "macroscopic" effects (i.e. the track length dependence). This improves the PID performance in terms of *separation power* to distinguish different classes of particles and reduces the effects due to the *correlations* between the $dE/dx$ response of tracks. Understanding the $dE/dx$ correlations is crucial to avoid bias in the estimate of physical observables.

## 2 Data sample

To extract the Universal Curves and to model the templates of the $dE/dx$ response we used $D^\star$-tagged $D^0 \to K^-\pi^+$ decays for pions and kaons, and $\Lambda \to p\pi^-$ decays for protons.

## 2.1 Pions and Kaons

We used a high-statistics and very pure sample of XFT-triggered kaons and pions from $D^{\star}$-tagged $D^0$ decays. The strong $D^{\star}$ decay unambiguously identifies the flavor of the $D^0$ meson, which is reconstructed in its Cabibbo-favored decay $D^0 \to K^-\pi^+$. The data sample used was collected between Dec 2004 (run 190697) and Sep 2011 (run 312510), from Period 1 to Period 38, by the Displaced-Tracks Trigger. We used the standard good run list following the prescription of the $B$-Group (Good Run list V45, `goodrun_b_bs_nocal_nomu.list`) and the integrated luminosity of the total sample is about 9.30 fb$^{-1}$. The reconstruction and the selection of the tagged $D^0 \to K^-\pi^+$ decays, used in this work, is described in detail in Refs. [3, 4]. We used the official version of BottomMods package (offline version 6.1.4, v90) and the datasets (on filecatalog) used are: `xbhdih`, `xbhdii`, `xbhdij`, `xbhdik`, `xbhdfm`, `xbhdfn`, `xbhdfp`. We decided not to use the `xbhdid` dataset because of some issues on the dE/dx in function of the runs distribution (see appendix A). We required generic `B_CHARM` triggers instead of the subsample listed in table 3 of Ref. [3]. The offline selection is summarized in tab. 1.

To select a very pure sample of charged pions and kaons the analysis has been restricted to candidates found within $\pm 8$ MeV from the world average $D^0$ mass [5], and within $\pm 0.8$ MeV from the world average $D^{\star +}$ mass [5]. It consists of about $2.7 \times 10^6$ $D^{*+} \to D^0\pi^+ \to [K^-\pi^+]\pi^+$ candidates. A $D^{\star +}$ signal is visible over a very low background that includes random triplets of tracks satisfying accidentally the selection requirements and random tracks combined with a real $D^0$ decay (fake $D^{\star +}$). The result is a sample of kaons and pions pure at about 99.07%, as shown in fig. 1(a).

## 2.2 Protons

We used a high-statistics sample of XFT-triggered protons from $\Lambda \to p\pi^-$ decays. These two-body decays are reconstructed with the same prescription of the $B^0_{(s)} \to h^+h^{'-}$ decays [7], and are collected using the same `B_PIPI` trigger paths. $\Lambda \to p\pi^-$ decays are volunteers in the `B_PIPI` triggers, because the pion in the final state does not satisfy the trigger requirements. This is due to the small energy available in the $\Lambda$ rest frame ($m_{\Lambda^0} - m_p - m_\pi \simeq 38$ MeV/$c^2$). For the same reasons as the $D^{\star}$ sample, we used the data sample collected between Dec 2004 (run 190697) and Sep 2011 (run 312510), from Period 1 to Period 38, by the Displaced-Tracks Trigger. We used the standard good run list following the prescription of the $B$-Group (Good Run list V45, `goodrun_b_bs_nocal_nomu.list`) and the integrated luminosity of the total sample is about 9.30 fb$^{-1}$. We used the official BStNtuples running over the following cdfpbnt datasets: `xbppjh`, `xbppji`, `xbpppj`, `xbppjk`, `xbppjp`, looking for $\Lambda \to p\pi^-$ candidates in the Lm-PPi block. The reconstruction and the selection of the $\Lambda \to p\pi^-$ decays is described in detail in Ref. [8].

The invariant $p\pi$-mass distribution of the resulting sample is shown in fig. 1(b), while the selection is summarized in tab. 2. A simple binned $\chi^2$-fit of the distribution to a double Gaussian function for the signal, over a straight line function for the background, provides an estimate of about $554 \times 10^3$ $\Lambda \to p\pi^-$ decays. The signal is centered at about 1115.79 GeV/$c^2$, with about 1.8 MeV/$c^2$ $\sigma$, and $\approx 472$ signal-to-background ratio at the peak. The kinematics allows a fully separation between $\Lambda^0 \to p\pi^-$ and $\overline{\Lambda}^0 \to \overline{p}\pi^+$.

To select a pure sample of charged protons (and soft pions) the analysis has been restricted to candidates found within $\pm 3.6$ MeV from the world average $\Lambda$ mass [5], It consists of about $518 \times 10^3$ $\Lambda \to p\pi^-$ candidates good for the dE/dx studies, pure at

| Tracks | Units | Requirement |
|---|---|---|
| Axial Si hits | – | $\geq 3$ |
| $90^\circ - z$ Si hits | – | $\geq 2$ |
| SA Si hits | – | $\geq 1$ |
| Axial COT hits | – | $\geq 10$ |
| Stereo COT hits | – | $\geq 10$ |
| Total COT hits | – | $\geq 40$ |
| dE/dx COT hits | – | $\geq 40$ |
| $p_{\mathrm{T}}$ | GeV/$c$ | $> 2.2$ |
| $\lvert\eta\rvert$ | – | $< 1.0$ |
| $\lvert d_0\rvert$ | $\mu$m | [100, 1000] |
| $D^0$ candidates | | |
| Has Primary Vertex | – | true |
| $q(1) \times q(2)$ | $e^2$ | $-1$ |
| $L_{\mathrm{T}}$ | $\mu$m | $> 200$ |
| $\sum p_{\mathrm{T}}$ | GeV/$c$ | $> 4.5$ |
| $\lvert d_0\rvert$ | $\mu$m | $< 100$ |
| $\chi^2$ | – | $< 30$ |
| $\chi^2_{xy}$ | – | $< 15$ |
| $\lvert\eta\rvert$ | – | $< 1.0$ |
| $\Delta\varphi_0$ | Degrees | [2°, 90°] |
| $m_{\pi\pi}$ | GeV/$c^2$ | [1.8, 2.4] |
| Soft Pion | | |
| $\lvert z_0\rvert$ | cm | $< 1.5$ |
| $\lvert d_0\rvert$ | cm | $< 0.06$ |
| $p_{\mathrm{T}}$ | GeV/$c$ | $> 0.4$ |
| $\lvert\eta\rvert$ | – | $< 1.0$ |
| Total COT hits | – | $\geq 30$ |
| dE/dx COT hits | – | $\geq 40$ |
| Total Si hits | – | $\geq 2$ |

Table 1: Summary of the selection cuts for $D^0 \to h^+h'^-$ decays from $D^{*+} \to D^0\pi^+$. Variables names are self-explanatory.

99.38%, as shown in fig. 1(b).

## 3 Check of track-based calibration

The first step is to check that the $dE/dx$ calibration [2], performed up to P17 (about 3 fb$^{-1}$), can be extended up to P38 (about 9.3 fb$^{-1}$) without compromising the performances in separating different classes of particles. Thus we applied the calibration following the standard prescriptions as described in Ref. [2], using the official "`DeDx2008_funcs.h`" and "`DeDx2008_funcs.C`" functions. We plotted the corrected $dE/dx$ for pions, kaons and protons as a function of the following macroscopic observables: run number, number of $dE/dx$ hits, instantaneous luminosity, pseudorapidity, azimuthal angle and secance. The distributions for charged pions and kaons coming from $D^0 \to K^-\pi^+$ decays are shown in fig. 2, while those for protons and pions coming from $\Lambda \to p\pi^-$ decays are shown in fig. 3.

| Quantity of the track | Units | Requirement |
|---|---|---|
| $p_{\mathrm{T}}(p)$ | GeV/$c$ | $> 2.0$ |
| $\lvert\eta(p)\rvert$ | – | $< 1.0$ |
| $\lvert d_0(p)\rvert$ | $\mu$m | [100, 1000] |
| Quantity of the candidate | | |
| $q(p) \times q(\pi)$ | $e^2$ | $-1$ |
| $d_0(p) \times d_0(\pi)$ | $\mu\mathrm{m}^2$ | $< 0$ |
| $\mathrm{corr}((d_0(p), d_0(\pi)))$ | $\mu$m | $< 51$ |
| $L_{\mathrm{T}}$ | cm | [0.5, 2.2] |
| $\sum p_{\mathrm{T}}$ | GeV/$c$ | $> 1.1$ |
| $\lvert d_0\rvert$ | $\mu$m | $< 70$ |
| $\lvert z_0(p) - z_0(\pi)\rvert$ | cm | $< 2$ |
| $\chi^2_{\mathrm{T}}$ | – | $< 10$ |
| $m_{p\pi}$ | GeV/$c^2$ | [1.10, 1.13] |
| $m_{\pi\pi}$ | GeV/$c^2$ | [0.35, 1.5] |
| $\lvert m_{\pi\pi} - m_{K^0_s}\rvert$ | GeV/$c^2$ | $> 0.0126$ |

Table 2: Summary of the selection used to reconstruct the $\Lambda \to p\pi^-$ decays. $\mathrm{corr}((d_0(p), d_0(\pi)))$ is a variable related to the correlation between the proton and the pion impact parameters. It selects a region in the two-dimensional space $((d_0(p), d_0(\pi)))$, for more details see [10].

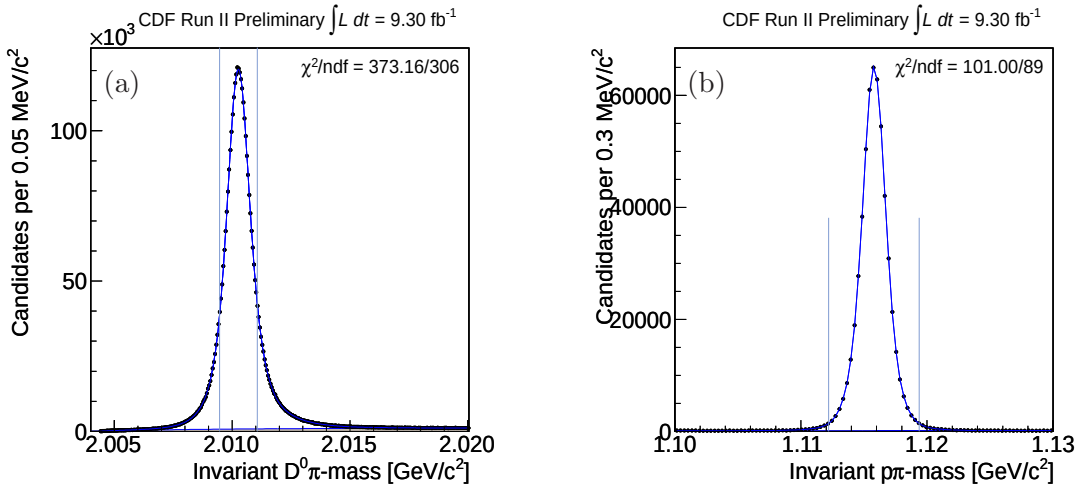


Figure 1: Invariant $D^0\pi$-mass for $D^{*+} \to D^0\pi^+ \to [K^-\pi^+]\pi^+$ decays (a) and invariant $p\pi^-$-mass for $\Lambda \to p\pi^-$ decays (b).

The distributions for XFT-triggered pions, kaons and protons do not show any relevant issues and are compatible with the same distributions shown in Ref. [2]. The calibration seems to be satisfactory when it is applied over the all data sample, up to P38. A small disagreement in the distribution of number of dE/dx hits versus dE/dx is visible in fig. 3. The distribution has a small jump towards higher values after n=60 hits. This is due to the change in the conditions on hits beginning from run 228819. From this run on, the SL0 and SL1 were disabled. Furthermore, from period 18 on, the instantaneous luminosity had

a major increase. Higher luminosity can cause more overlaps and fakes resulting in fewer good hits. So the mean number of dE/dx hits is lower with respect to the previous periods, causing this small discrepancy. This effect is also present in the $D^0 \to K^-\pi^+$ sample, but it is less emphasized, because the increasing in luminosity is lower than respect to the $\Lambda \to p\pi^-$ sample.

Some small issues can also be observed for non-triggered soft pions. The calibration has been done only for triggered tracks, and some difficulties can raise when it is applied to very low momentum tracks, below 2 GeV/$c$. For instance we expect that the correction as a function of the secance does not accurately work for low momentum tracks since it has been done only for triggered tracks. However this is not a main stopper for the aim of this work, since we are interested in modeling the $dE/dx$ response only for triggered tracks. The low momentum pions are a different chapter and are beyond our current scope. We just expect to get a larger correlation between protons and pions from $\Lambda \to p\pi^-$ with respect to that one between pions and kaons from $D^0 \to K^-\pi^+$ decays.

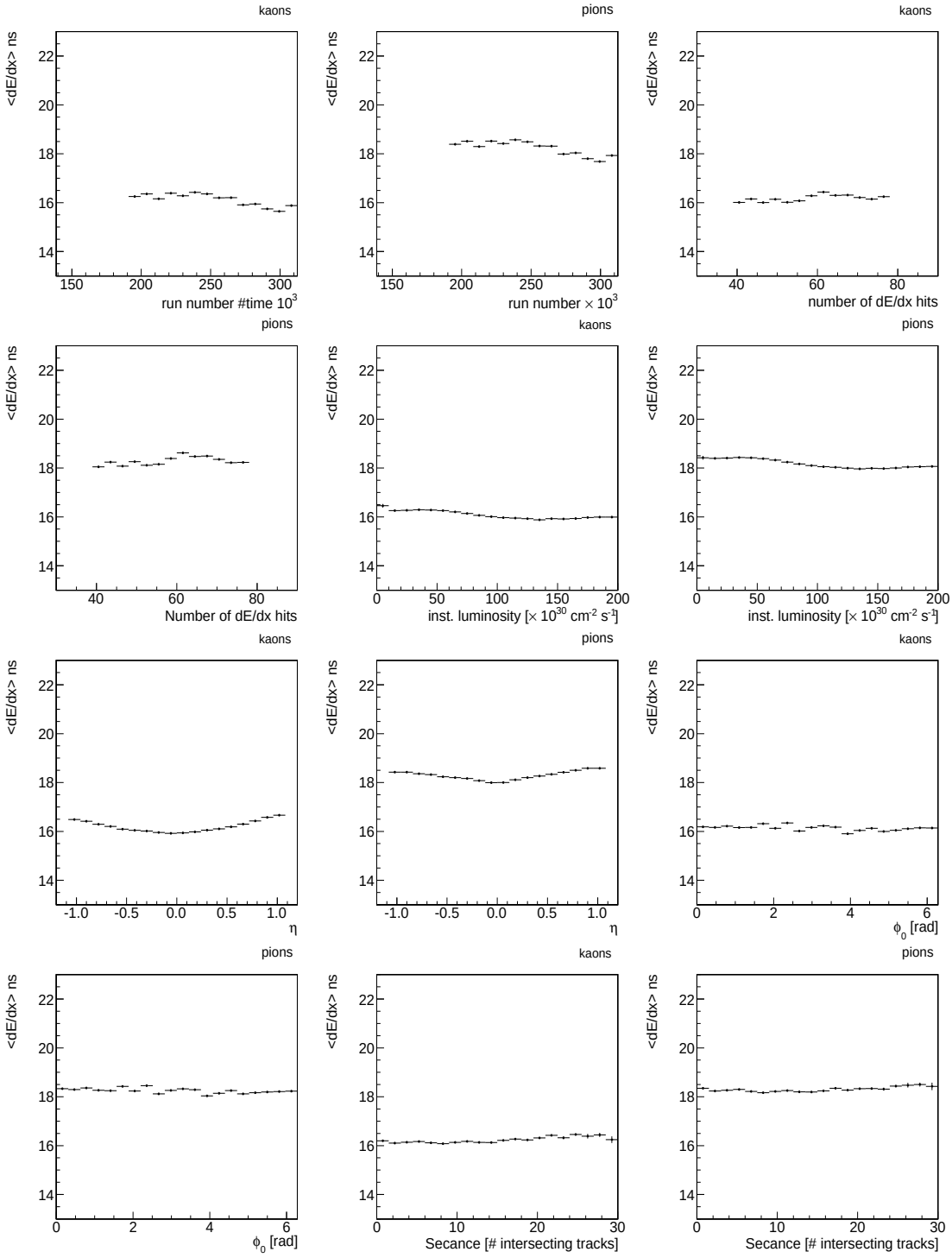


Figure 2: Corrected dE/dx for pions and kaons from $D^0 \to K^-\pi^+$ decays.

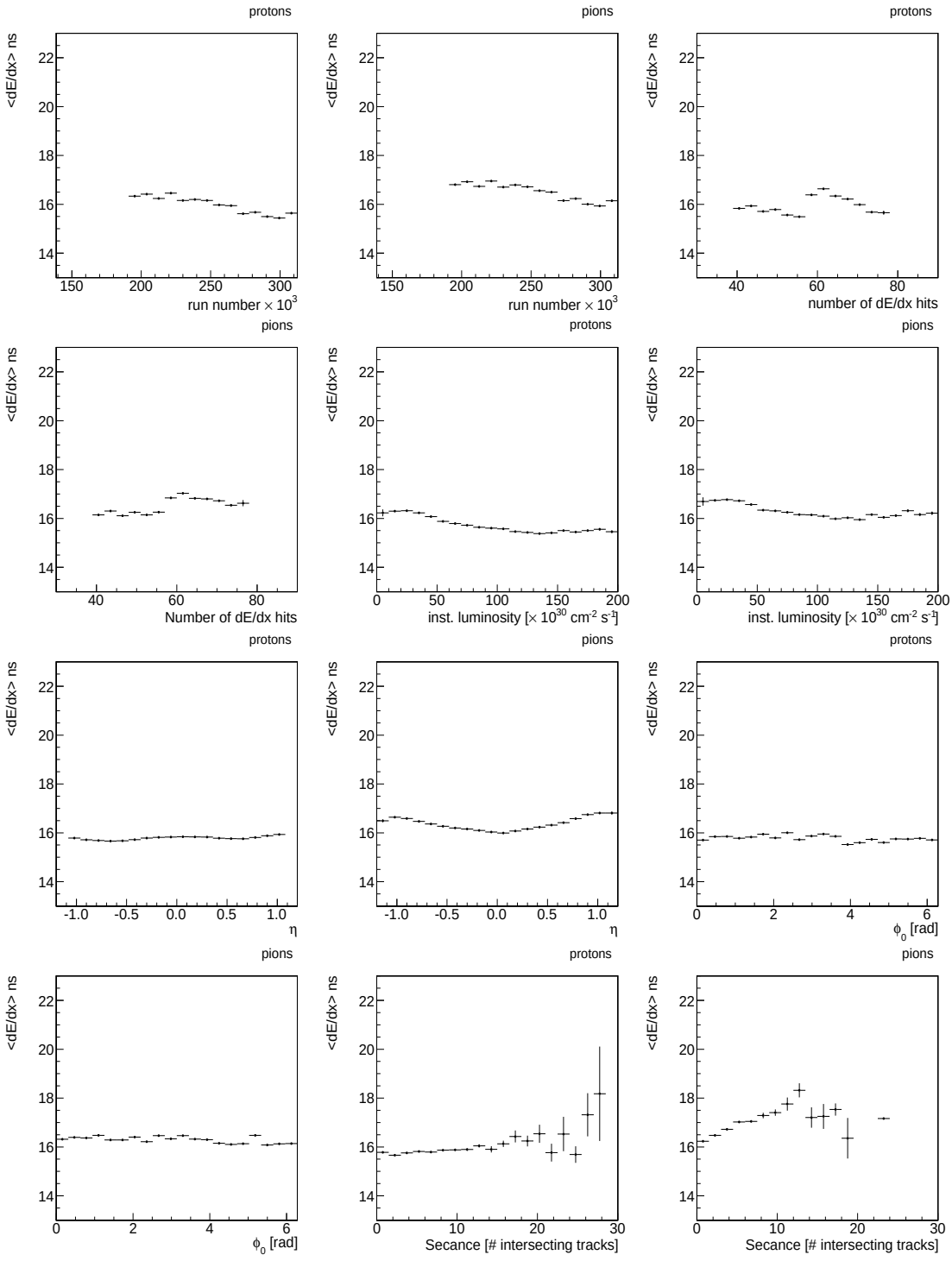


Figure 3: Corrected dE/dx for pions and protons from $\Lambda \to p\pi^-$ decays.

# 4 Universal Curves

The average total energy-loss per unit length of a particle (heavier than the electron) of charge $q$ traversing a gas volume with velocity $c\beta$ is approximated by the Bethe-Bloch formula [11]

$$\left\langle \frac{dE}{dx} \right\rangle = \frac{4\pi N e^4}{m_e c^2 \beta^2} q^2 \left[ \ln \left( \frac{2 m_e c^2 \beta^2 \gamma^2}{I} \right) - \beta^2 - \frac{\delta(\beta)}{2} \right], \tag{1}$$

where $N$ is the electron density in the medium, $m_e$ ($e$) is the electron mass (charge), $I$ is the mean excitation energy of the medium atoms, and $\delta(\beta)$ is the correction that accounts for the density effect at high velocities. To a good approximation, the most probable $dE/dx$ value of a charged particle is a function of its velocity. If the momentum of the particle is measured, the mass can also be determined. In the COT, the signal induced on each sense-wire depends on the amount of ionization charge produced by the passage of the charged particle near the wire. It is measured in nanoseconds because it is encoded as the digital pulse-width between the leading and the trailing-edge time of the hit. Multiple samplings along the trajectory of the charged particle allow a more reliable estimation of $dE/dx$, which has usually a broad distribution. The COT samples a maximum of 96 $dE/dx$ measurements per track, from which a 80% truncated mean is calculated to avoid the adverse effect of long positive tails in the estimation of the average $dE/dx$.

The empirical equation that better models the COT average energy-loss as a function of velocity is the following variant of the Bethe-Bloch curve:

$$\left\langle \frac{dE}{dx} \right\rangle = \frac{1}{\beta^2} \left[ c_1 \ln \left( \frac{\beta\gamma}{b + \beta\gamma} \right) + c_0 \right] + a_1(\beta - 1) + a_2(\beta - 1)^2 + C, \tag{2}$$

with $a_i$, $b$, $c_j$, and $C$ parameters extracted from data. The above function has all the features that are present in the Bethe-Bloch curve (eq. (1)). The parameters $c_0$ and $c_1$ represent the intensities of the $1/\beta^2$ fall and of the relativistic rise. The parameter $b$ is associated with the COT gas properties, e. g., mean excitation energy of the gas atoms, etc.. The parameters $a_1$ and $a_2$ provide a further adjustment, especially in the low $\beta\gamma$ region.

Figures 4 and 5 show average values of the $dE/dx$ as a function of $\beta\gamma$, separately for pions, kaons, protons and soft pions and positively/negatively-charged particles. Fit of these curves (with $a_i$, $b$, $c_j$, and $C$ free parameters) with the empiric modification of the Bethe- Bloch curve in eq. (2) are overlaid (blue line). The old parameterizations are reported in appendix B.

Figure 6 shows the summary for universal curves as a function of the momentum for all kind of particles separated by charge.

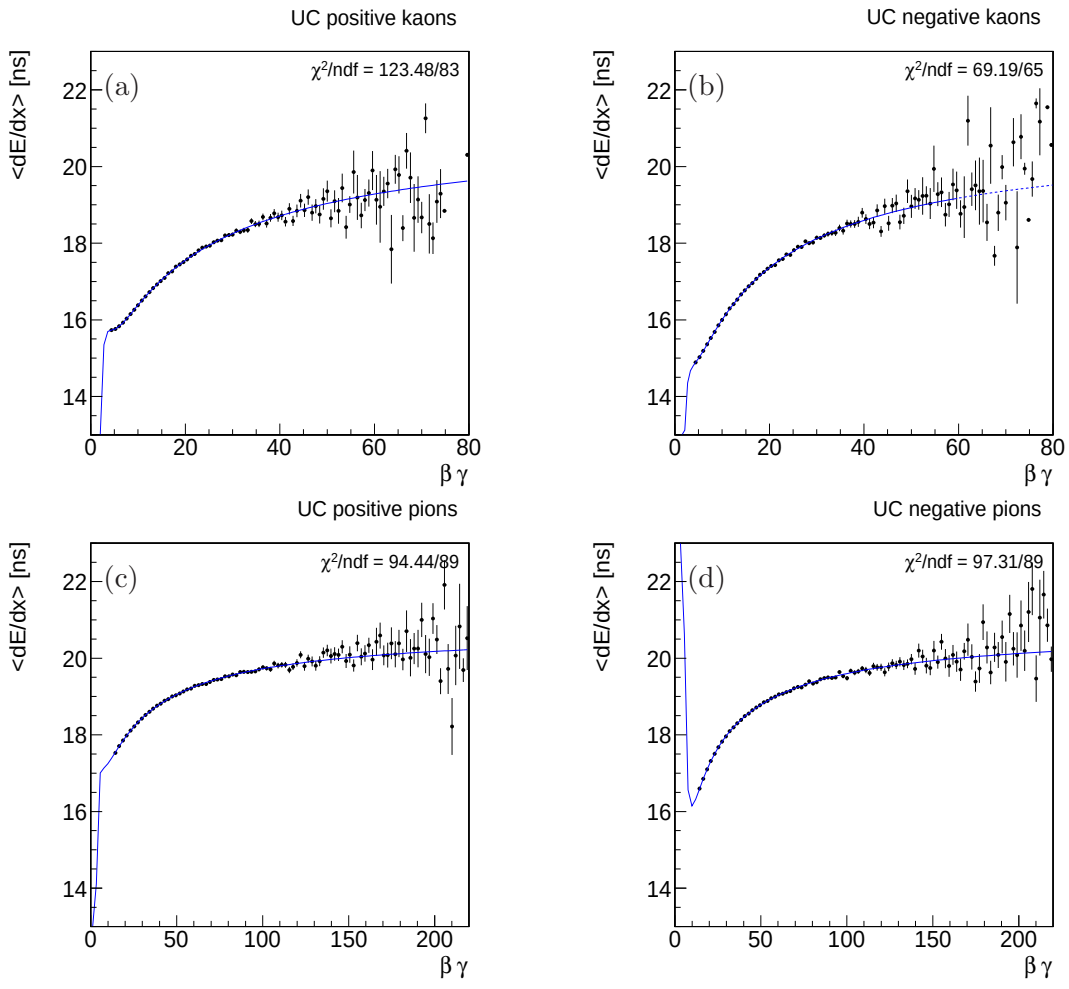


Figure 4: Parameterization (blue) of the Universal Curves for charged pions and kaons from $D^0 \to K^-\pi^+$ decays.

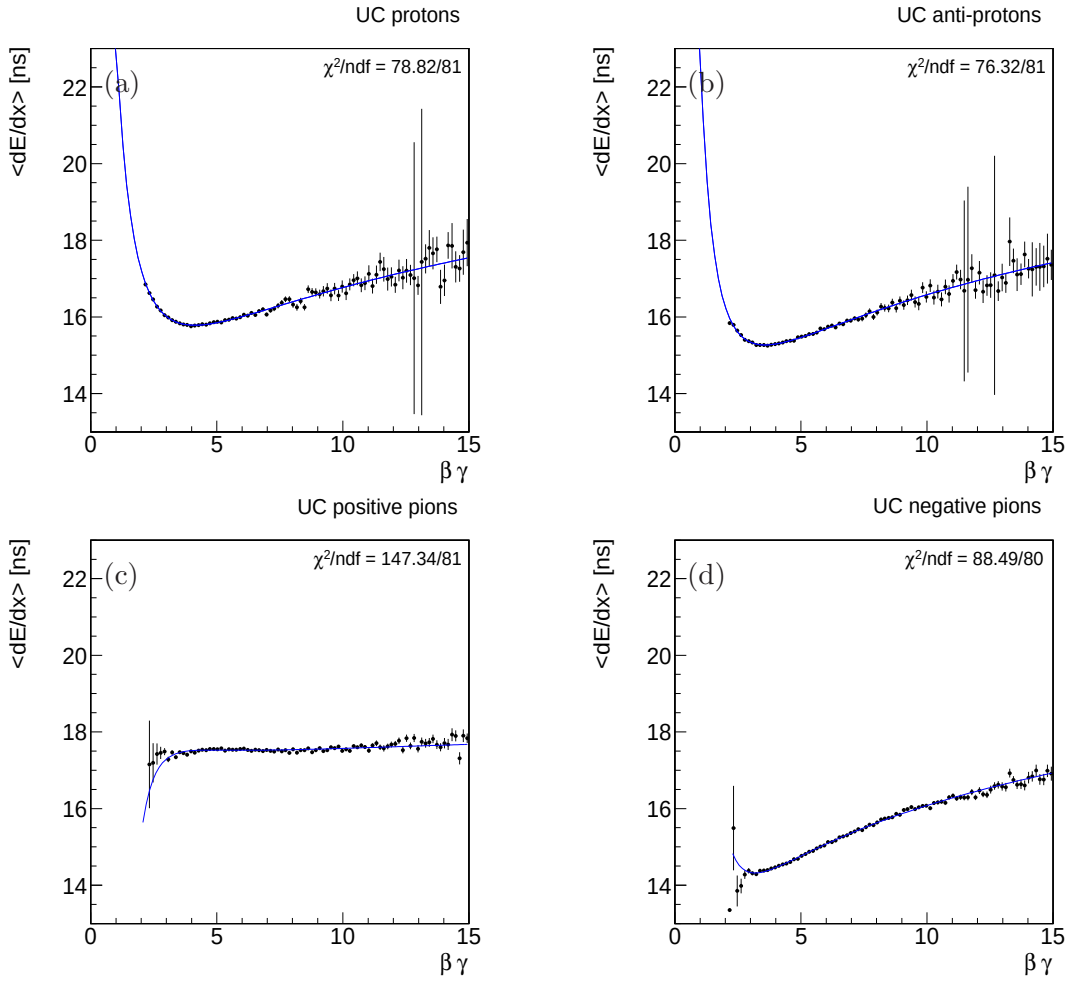


Figure 5: Parameterization (blue) of the Universal Curves for charged pions and protons from $\Lambda \to p\pi^-$ decays.

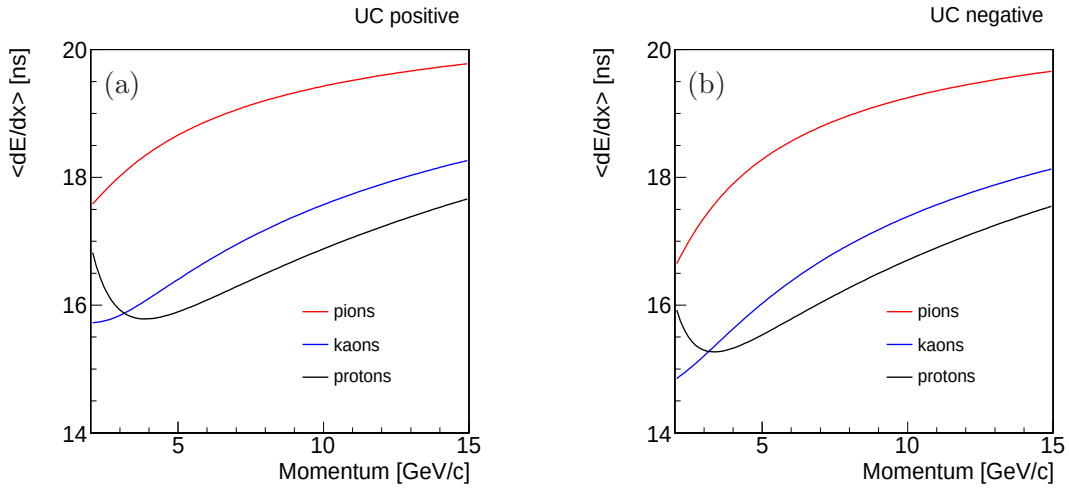


Figure 6: Universal curves as a function of particle momentum.

## 5 Separation power

The $dE/dx$ residual (in $m_A$ mass hypothesis) of a charged particle with momentum $p$ and observed specific energy-loss $dE/dx_{\rm obs}$, is defined as

$$\delta_A = \frac{dE}{dx}_{\rm obs} - \frac{dE}{dx}_A, \tag{3}$$

where $dE/dx_A$ is the expected $dE/dx$, determined from the function eq. (2) evaluated at $\beta\gamma = p/m_A$. The identification performance relies on the difference in the distributions of the $dE/dx$ residual between the classes of events to be identified. Such difference is generally expressed in terms of a *separation* between those distributions. We chose to use $dE/dx$ residuals with pion mass hypothesis, $\delta_\pi$, since no significant enhancements in separation were found by using other variables.

Following the approach described in Ref. [12] (see also Ref. [2] for details), the resulting separation between pions and kaons from the $D^0 \to K^-\pi^+$ decays is $1.44\sigma$ ($\sigma_f^{\rm best}/\sigma_f = 0.60\%$) for positively-charged particles, and $1.42\sigma$ ($\sigma_f^{\rm best}/\sigma_f = 59.3\%$) for negatively-charged particles, approximately constant in the momentum range of interest $2 \lesssim p \lesssim 20$ GeV/$c$. Since the separation power depends on the specific proportions among classes of events present in the sample, the above values hold only for samples with approximately equal contributions from pions and kaons. The performances obtained for a data sample of 9.3 fb$^{-1}$ are compatible (actually the same values) with those obtained in Ref. [13] for a data sample of 6 fb$^{-1}$. This result ensures that the $dE/dx$ response does not chance in time and that the calibration can be extended to all data sample without any issues.

## 6 Correlations

Figure 7 shows the distribution of the residual for kaons (with kaon hypothesis) as a function of the residual for pions (with pion hypothesis) and the same two-dimensional distribution of the residual for protons (with proton hypothesis) as a function of the residual for pions (with pions hypothesis).

A non-zero, positive correlation is visible from the shape of the distributions, corresponding to a correlation coefficient $\rho \simeq 8\%$ for kaons and pions from $D^0 \to K^-\pi^+$ decays and $\rho \simeq 11\%$ for protons and pions from $\Lambda \to p\pi^-$ decays.[1] This correlation is dangerous for the analyses using $dE/dx$ observables. While a small separation power only degrades the statistical uncertainty on the relative fractions of the different signal modes, a large correlation strongly biases the central values. Therefore this effect must be carefully studied and parameterized.

With an ideal PID detector, no correlation is expected between independent measurements. A non-vanishing correlation indicates the presence of residual $dE/dx$ gain variations from event to event. The sources of this correlation can be divided into two groupes:

**Global effects** – these are all the effects unrelated to the kinematics. Suppose the $dE/dx$ shows gain variations as a function of the instantaneous luminosity: $\frac{dE}{dx} = \frac{dE}{dx}(\beta\gamma, \mathcal{L})$. Then, since the kaon and the pion from a $D^0$ decay are reconstructed in the same

[1] The correlation coefficient in this case is $\rho = \frac{E[\delta_\pi \times \delta_{K(p)}] - E[\delta_\pi] \times E[\delta_{K(p)}]}{\sigma_{\delta_\pi} \times \sigma_{\delta_{K(p)}}}$, in which $E[x]$ indicates the expected value of $x$, and $\sigma$ are sample standard-deviations.

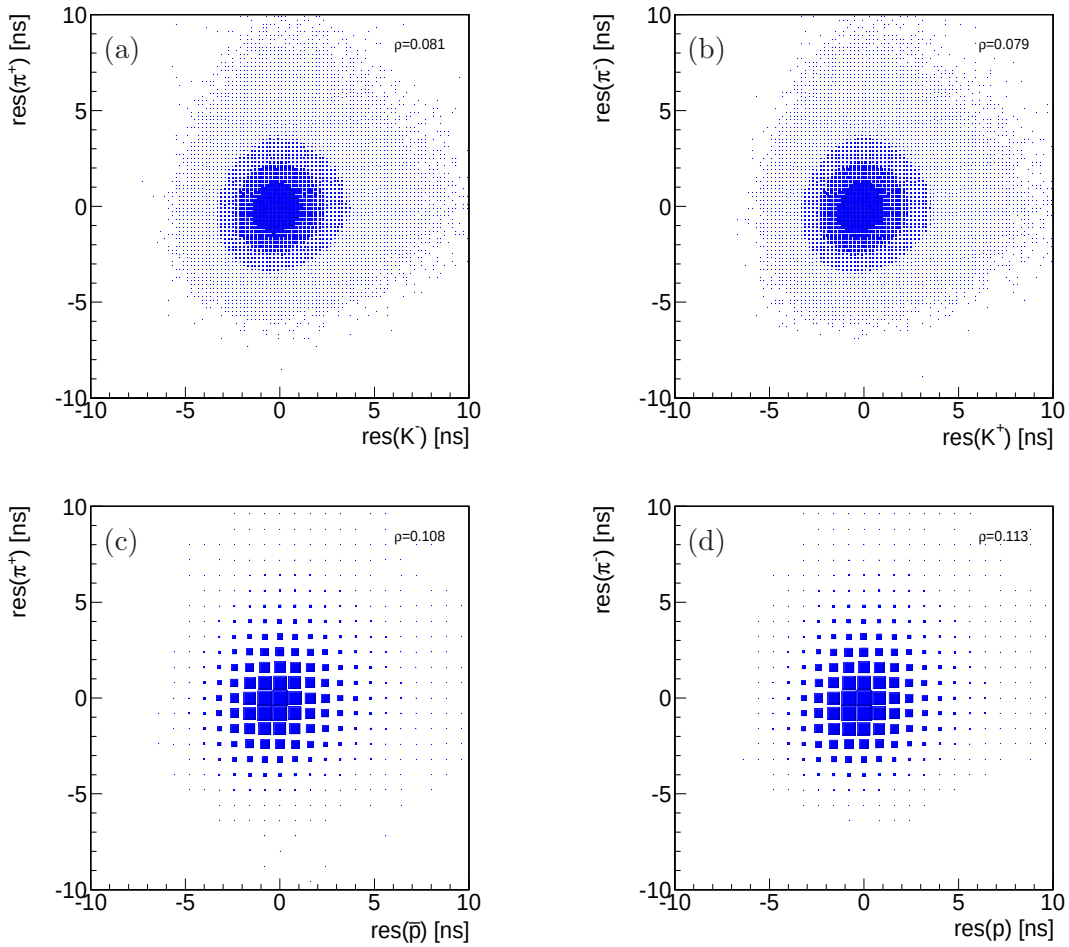


Figure 7: Residual for pions (with pion hypothesis) as a function of the residual for kaons (with kaon hypothesis) (a,b). Residual for pions (with pion hypothesis) as a function of the residual for protons (with proton hypothesis) (c,d).

event (e. g., in the same conditions of luminosity), their observed $dE/dx$ would appear correlated by the common dependence on luminosity. This may apply to a variety of global variables, such as time, pressure or temperature of the gas, and so forth.

**Local effects** – these are all effects related to kinematics. Suppose that the $dE/dx$ shows gain variations as a function of the azimuthal angle of emission of the particle: $\frac{dE}{dx} = \frac{dE}{dx}(\beta\gamma, \varphi_0)$. Then, since the azimuthal angle of a kaon and a pion from a $D^0$ decay are correlated by the kinematic of the decay and by the selection cuts, their observed $dE/dx$ would become correlated. This may apply to a variety of local variables, such as $\eta$, $z_0$, hit multiplicity, etc.

We investigated the combined effect of all possible residual gain variations by allowing for a generic, time-dependent common-mode fluctuation $c(t)$ that affects and correlates the observed $dE/dx$ values of the tracks in the event. In particular, we extracted the variance ($\sigma_c^2$) of the distribution of the common mode, as an estimator of the size of the correlation. We denote the probability distribution of the $dE/dx$ residual for pions (with

pion mass-hypothesis) as $\wp_\pi(\delta_\pi)$, with standard deviation $\sigma_\pi$. A similar notation is used for kaons. If $\delta_\pi$ and $\delta_K$ were independent variables, the probability distribution of their sum $(\delta_K + \delta_\pi)$ would satisfy

$$\wp(\delta_\pi + \delta_K) = \wp_\pi(\delta_\pi) * \wp_K(\delta_K), \tag{4}$$

in which the symbol $*$ indicates the Fourier convolution product.[2] Similarly, their difference $\delta_\pi - \delta_K$ would be distributed as

$$\wp(\delta_\pi - \delta_K) = \wp_\pi(\delta_\pi) * \wp_{-K}(-\delta_K), \tag{5}$$

where $\wp_{-K}(-\delta_K)$ is the distribution of the negative residual for kaons $(\frac{dE}{dx}_K - \frac{dE}{dx}_{\rm obs})$, whose variance satisfies the condition $\sigma^2_K = \sigma^2_{-K}$. Since the variance of a convolution product is the sum of variances of the convoluted distributions, the standard deviations of the distributions of sum and difference are equal:

$$\sigma_{\pi+K} = \sigma_{\pi-K} = \sqrt{\sigma^2_\pi + \sigma^2_K}. \tag{6}$$

On the other hand, if the two residuals are correlated by a common-mode fluctuation, the observed residual ($\delta^{\rm obs}$) is written as the sum of the intrinsic, uncorrelated residual with the common-mode shift:

$$\delta^{\rm obs}_\pi = \delta_\pi + c \quad \text{and} \quad \delta^{\rm obs}_K = \delta_K + c. \tag{7}$$

Therefore, the sum of the observed residuals, $\delta^{\rm obs}_\pi + \delta^{\rm obs}_K = \delta_\pi + \delta_K + 2c$, is distributed as

$$\wp(\delta^{\rm obs}_\pi + \delta^{\rm obs}_K) = \wp_\pi(\delta_\pi) * \wp_K(\delta_K) * \wp_c(2c), \tag{8}$$

whereas their difference, $\delta^{\rm obs}_\pi - \delta^{\rm obs}_K = \delta_\pi + c - \delta_K - c = \delta_\pi - \delta_K$, is distributed as

$$\wp(\delta^{\rm obs}_\pi - \delta^{\rm obs}_K) = \wp_\pi(\delta_\pi) * \wp_{-K}(-\delta_K). \tag{9}$$

Equations (8) and (9) show that, in presence of a common mode, the sum of residuals has greater variance than their difference, $\sigma^2_{\pi+K} > \sigma^2_{K-\pi}$. The standard deviation of the correlation is easily obtained:

$$\sigma_c = \frac{1}{2}\sqrt{\sigma^2_{\pi+K} - \sigma^2_{\pi-K}}. \tag{10}$$

Following eq. (10), we used the distributions of sum and difference of the observed residual to estimate the magnitude of time-dependent common modes. The same relationship holds for $\Lambda \to p\pi^-$ decays, then the standard deviation of the time-dependent common-mode is in this case:

$$\sigma_c = \frac{1}{2}\sqrt{\sigma^2_{\pi+p} - \sigma^2_{\pi-p}}. \tag{11}$$

We extracted $\sigma_c$ for the four possible combinations, and the results are reported on tab. 3. The standard deviation of correlation distribution extracted for kaons and pions from $D^0 \to K^-\pi^+$ decays is $\sigma_c = 0.44$ ns, in good agreement with the previous estimate done in Ref. [2]. This result, along with the non degraded performances in separation, tells us that the calibration can be extended up to P38 without any particular issues. For protons and pions from $\Lambda \to p\pi^-$ decays $\sigma_c = 0.55$ ns which is larger than the value obtained from pions and kaons from $D^0 \to K^-\pi^+$. This is widely expected, since the calibration does not work accurately for low momentum pions. This is automatically included in the standard deviation of the correlation distribution.

[2] Henceforth, "convolution" always denote the Fourier convolution product.

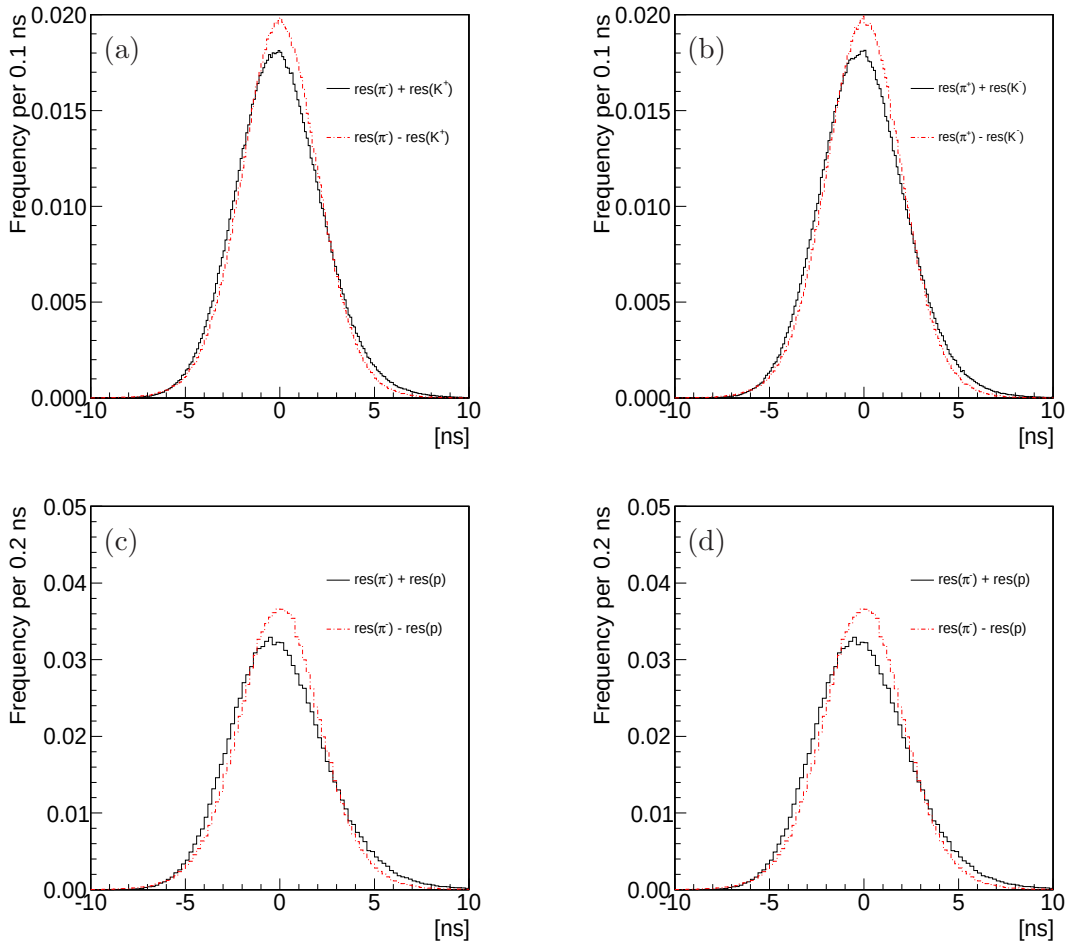


Figure 8: Distribution of the sum (black continuous line) and difference (red dashed line) of residuals for a kaon/proton (in kaon/proton hypothesis) and a pion (in pion hypothesis) from $D^0 \to K^-\pi^+$ and $\Lambda \to p\pi^-$ decays.

| | $\sigma_{\pi+K}$ | $\sigma_{\pi-K}$ | $\sigma_c$ |
|---|---|---|---|
| $D^0 \to K^-\pi^+$ | 2.28 | 2.11 | 0.44 |
| $\overline{D}^0 \to K^+\pi^-$ | 2.28 | 2.11 | 0.43 |
| | $\sigma_{\pi+p}$ | $\sigma_{\pi-p}$ | $\sigma_c$ |
| $\Lambda \to p\pi^-$ | 2.53 | 2.28 | 0.55 |
| $\overline{\Lambda} \to \overline{p}\pi^+$ | 2.52 | 2.28 | 0.54 |

Table 3: Standard deviation of the sum and difference of residual distributions (see text) and standard deviation of the extracted correlation. Units are in nano seconds.

# 7 Model of the $dE/dx$ distributions

Using the $dE/dx$ information in a Likelihood fit requires modeling the distributions of the desired observables. It is convenient to stress the difference between *observed* $dE/dx$ quantities, i. e., those affected by common-mode fluctuations, and *intrinsic* quantities,

the quantities which would have been observed if the correlations were not present. Since the intrinsic residuals and the correlation are, by construction, independent variables (see eq. (7)), the (known) distribution of the observed residuals is the convolution of their unknown distributions:

$$\wp(\delta^{\rm obs}) = \wp(\delta + c) = \wp(\delta) * \wp(c). \tag{12}$$

The model of the intrinsic residuals, $\wp(\delta)$, and of the correlations, $\wp(c)$, is extracted from the distributions of the observed residuals, $\wp(\delta^{\rm obs})$, of pions and kaons from $D^0$ decays. We expand each term of the right-hand side of eq. (12) in sum of Gaussian distributions, and we fit the distributions of the observed residuals to get the unknown parameters. In practice, the first three terms of the expansion are sufficient to model accurately the intrinsic residuals and correlations:

$$\wp_K(\delta_K) = q' \cdot \mathscr{G}_{K'}(\delta_K) + q'' \cdot \mathscr{G}_{K''}(\delta_K) + (1 - q' - q'') \cdot \mathscr{G}_{K'''}(\delta_K) \tag{13}$$

$$\wp_\pi(\delta_\pi) = p' \cdot \mathscr{G}_{\pi''}(\delta_\pi) + p'' \cdot \mathscr{G}_{\pi''}(\delta_\pi) + (1 - p' - p'') \cdot \mathscr{G}_{\pi'''}(\delta_\pi) \tag{14}$$

$$\wp_c(c) = r \cdot \mathscr{G}_{c'}(c) + (1 - r) \cdot \mathscr{G}_{c''}(c) \tag{15}$$

where we use the following notation for the Gaussian distribution:

$$\mathscr{G}_s(x) = \mathscr{G}(x; \mu_s, \sigma_s) = \frac{1}{\sigma_s\sqrt{2\pi}} e^{-\frac{(x-\mu_s)^2}{2\sigma_s^2}}.$$

Independent parameterizations are assumed for the distributions of intrinsic residuals for positively and negatively-charged particles. Mean ($\mu$), variance ($\sigma^2$) and fraction of each Gaussian are determined with a simultaneous, binned ML fit of the following combinations of observed residuals:

$$\wp_K(\delta_K^{\rm obs}) = \wp(\delta_K) * \wp(c) = (\mathscr{G}_{K'} + \mathscr{G}_{K''} + \mathscr{G}_{K'''}) * (\mathscr{G}_{c'} + \mathscr{G}_{c''}) \tag{16}$$

$$\wp_\pi(\delta_\pi^{\rm obs}) = \wp(\delta_\pi) * \wp(c) = (\mathscr{G}_{\pi'} + \mathscr{G}_{\pi''} + \mathscr{G}_{\pi'''}) * (\mathscr{G}_{c'} + \mathscr{G}_{c''}) \tag{17}$$

$$\wp(\delta_\pi^{\rm obs} + \delta_K^{\rm obs}) = (\mathscr{G}_{\pi'} + \mathscr{G}_{\pi''} + \mathscr{G}_{\pi'''}) * (\mathscr{G}_{K'} + \mathscr{G}_{K''} + \mathscr{G}_{K'''}) * (\mathscr{G}_{2c'} + \mathscr{G}_{2c''}) \tag{18}$$

$$\wp(\delta_\pi^{\rm obs} - \delta_K^{\rm obs}) = (\mathscr{G}_{\pi'} + \mathscr{G}_{\pi''} + \mathscr{G}_{\pi'''}) * (\mathscr{G}_{-K'} + \mathscr{G}_{-K''} + \mathscr{G}_{-K'''}), \tag{19}$$

where the relative normalization factors $(p, q, r)$ is included in the fit, but omitted above for a clearer notation. If in the equations above (eqs. (13)–(19)) we replace the kaon index ($K$) with the proton index ($p$) we obtain the equivalent relations to model the probability density functions of protons and pions from $\Lambda \to p\pi^-$ decay. In this case we parameterize a different correlation function with respect to the $D^0 \to K^-\pi^+$ case since we used a different sample.

The technique used to extract the parameters of the $dE/dx$ templates, of the intrinsic residuals and correlation, is based on an iterative method of one-dimensional binned fits of the distributions of $\delta_\pi^{\rm obs}$, $\delta_K^{\rm obs}$, $\delta_\pi^{\rm obs}+\delta_K^{\rm obs}$ and $\delta_\pi^{\rm obs}-\delta_K^{\rm obs}$. The details of the parameterization can be found in [14, 15, 16, 17].

Figures 9–12 show a satisfactory agreement between the chosen model and the distributions of the observed residuals and correlations. Although we allow for independent residual distributions for kaons, pions and protons (negative and positive particles) the extracted shapes are similar, all showing non-Gaussian positive tails. The differences between the residuals of positively and negatively-charged particles are tiny.

We extracted two models for the correlation function: one from the $D^0 \to K^-\pi^+$ sample and the other one from the $\Lambda \to p\pi^-$ sample. Both models show a non negligible correlation, as expected from the distributions of the sum and the difference of the residuals. The correlation function extracted from pions and kaons from $D^0 \to K^-\pi^+$ decays has an average mean value $\mu \approx 0$ ns and a RMS $\sigma \approx 0.44$ ns, while for the correlation extracted from protons and pions from $\Lambda \to p\pi^-$ decays we obtain $\mu \approx 0$ ns and a RMS $\sigma \approx 0.56$ ns.

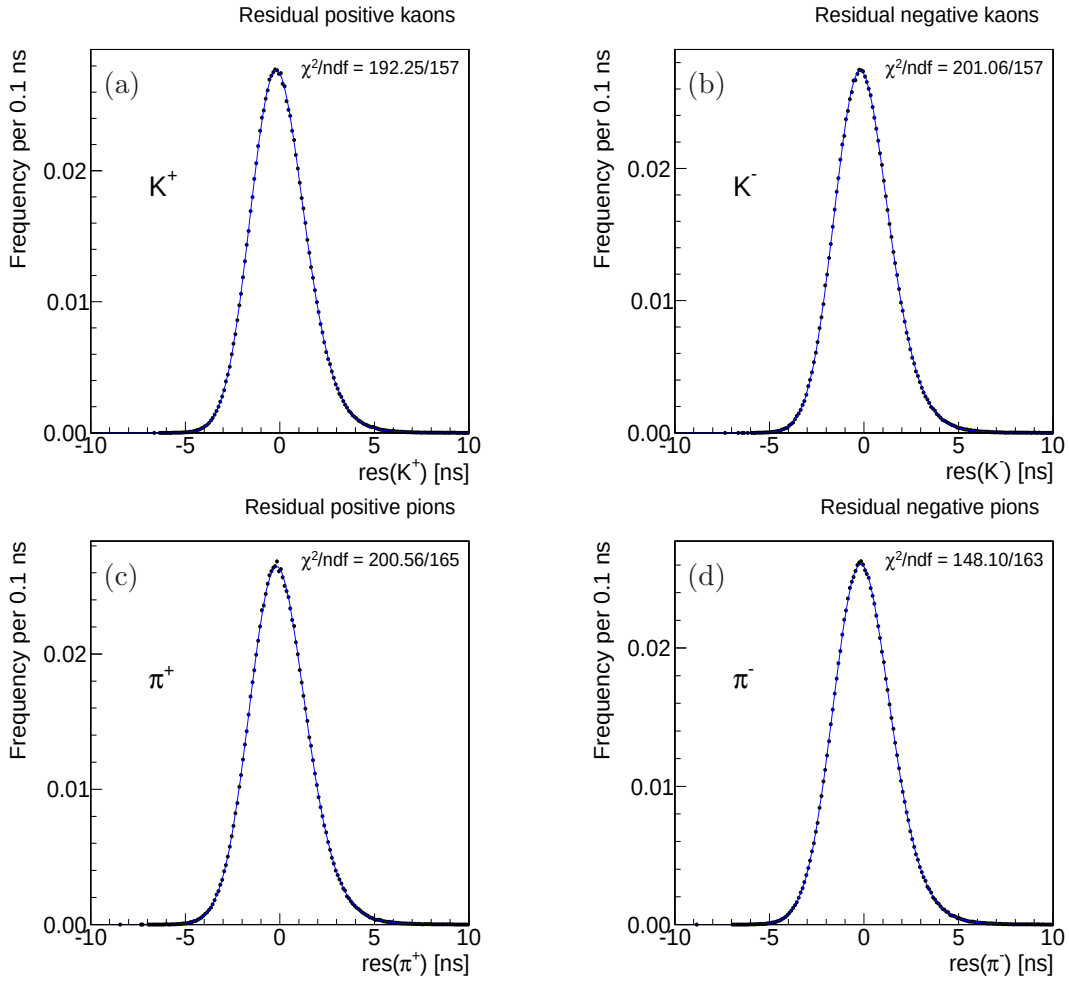


Figure 9: Distribution of observed $dE/dx$ residual ($\wp(\delta^{\rm obs}) = \wp(\delta + c) = \wp(\delta) * \wp(c)$), for kaons (with kaon mass hypothesis) (a,b), for pions (with pion mass hypothesis) (c,d) The results of the fit to the functions in eq. (16) and eq. (17) are overlaid (blue, solid line).

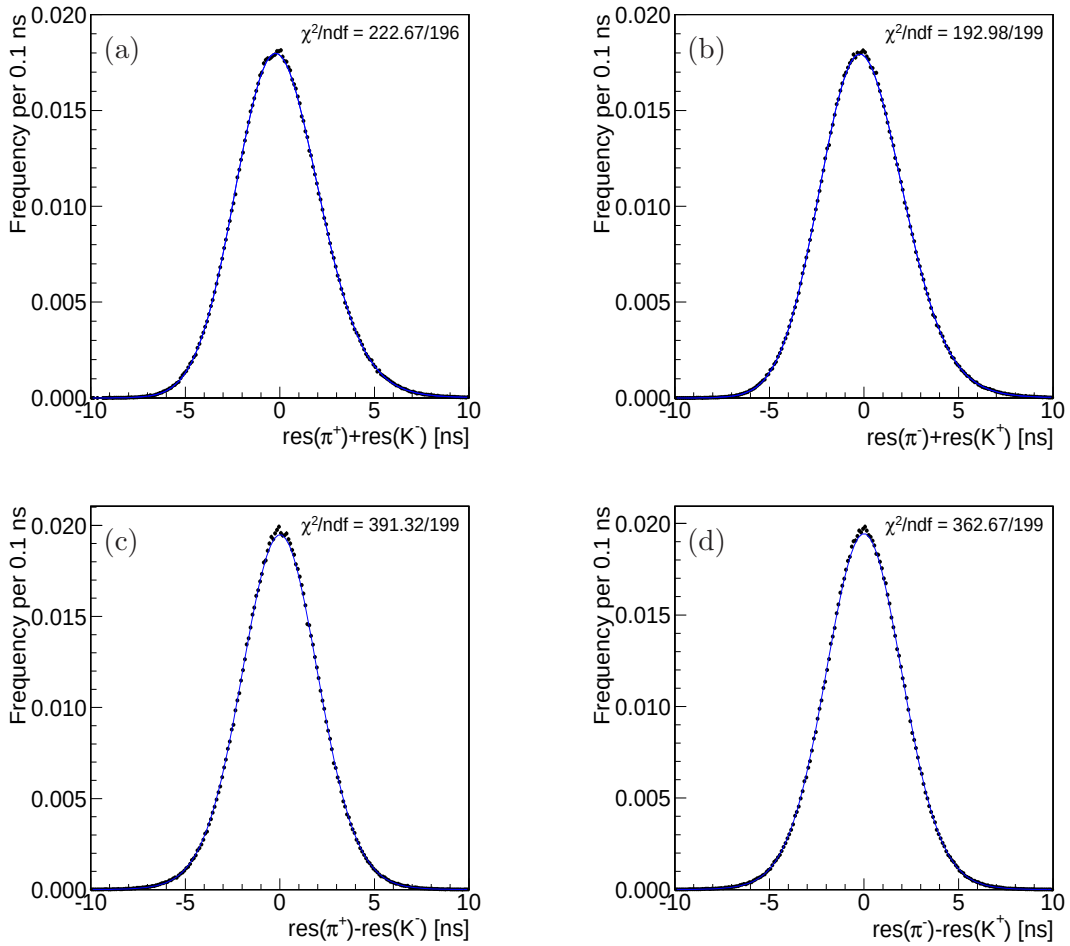


Figure 10: Distribution of the sum (a,b) and the difference (b,d) of the residuals for a kaon (in kaon hypothesis) and a pion (in pion hypothesis) from $D^0 \to K^-\pi^+$ decays. The results of the fit to the functions in eq. (18) and eq. (19) are overlaid (blue, solid line).

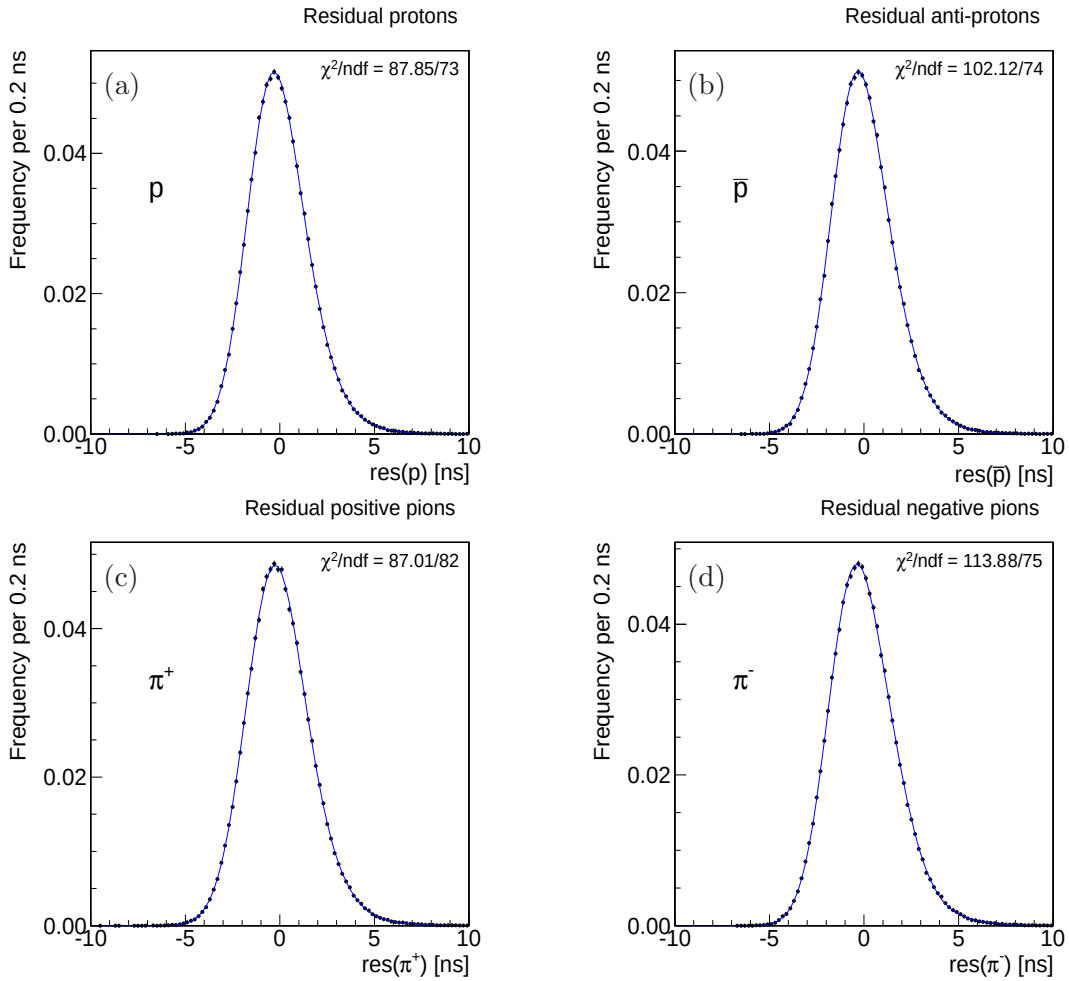


Figure 11: Distribution of observed $dE/dx$ residual ($\wp(\delta^{\rm obs}) = \wp(\delta + c) = \wp(\delta) * \wp(c)$), for protons (with protons mass hypothesis) (a,b), for pions (with pion mass hypothesis) (c,d) The results of the fit to the functions in eq. (16) and eq. (17), where $K \to p$, are overlaid (blue, solid line).

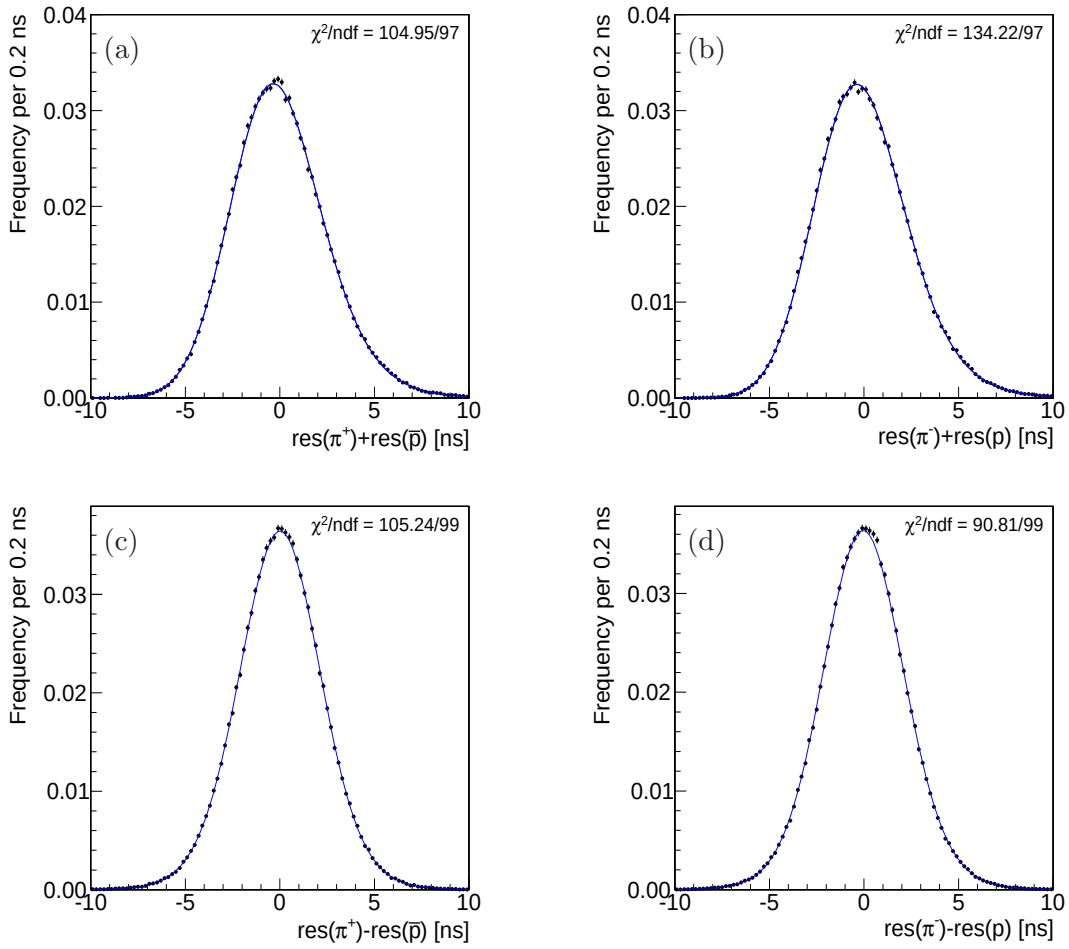


Figure 12: Distribution of the sum (a,b) and the difference (c,d) of residuals for a proton (in proton hypothesis) and a pion (in pion hypothesis) from $\Lambda \to p\pi^-$ decays. The results of the fit to the functions in eq. (18) and eq. (19), where $K \to p$, are overlaid (blue, solid line).

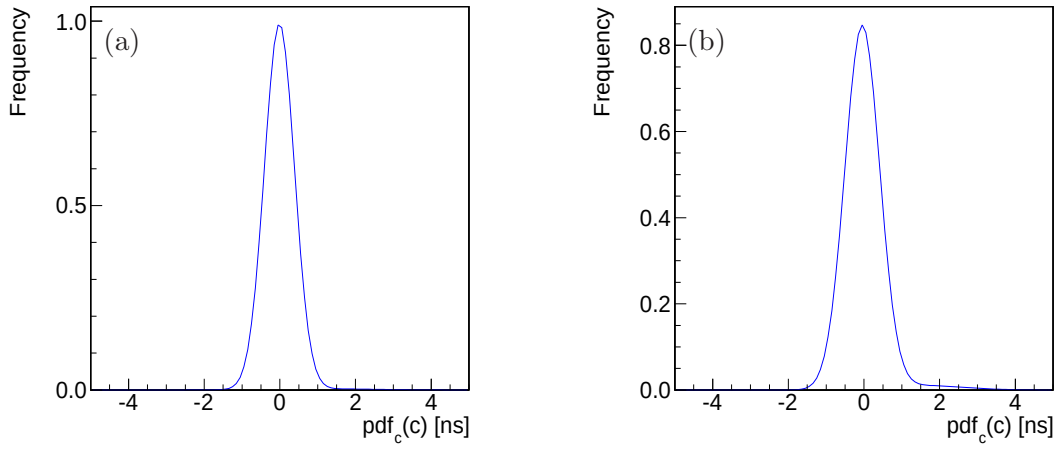


Figure 13: Correlation probability density functions for pions and kaons from $D^0 \to K^-\pi^+$ decays (a), for pions and protons from $\Lambda \to p\pi^-$ decays (b).

### 7.1 Comparison between residual p.d.f.

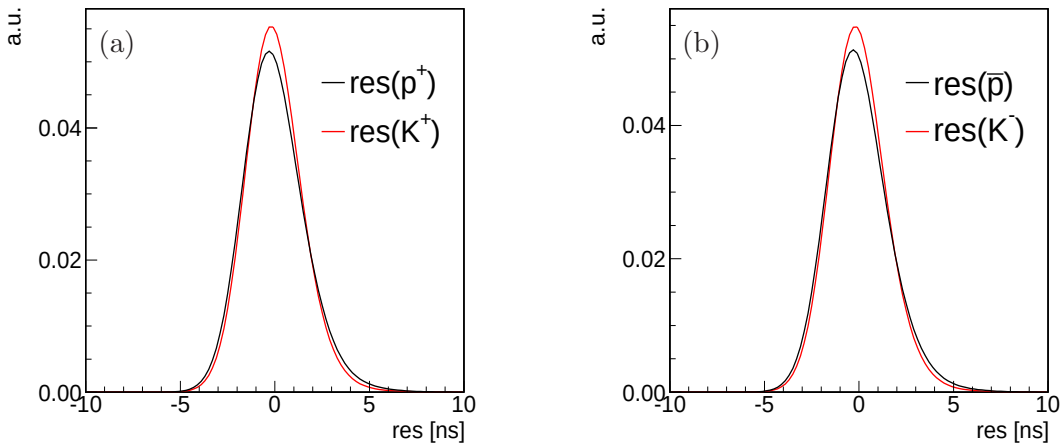


Figure 14: Residual probability density functions for kaons from $D^0 \to K^-\pi^+$ decays and for pions and protons from $\Lambda \to p\pi^-$ decays. Positively (a) and negatively (b) charged particles.

Figure 14 shows the difference between kaon and proton residuals. The kaon residuals have a lower RMS with respect to the proton residuals. This small effect can be due to the hardship of modeling the non-triggered soft pions.

## 8 Conclusions

We have produced an updated set of universal curves for charged pions, kaons and protons for analyses with 9.3 fb$^{-1}$ of data, corresponding to data collected from P1 to P38. The $dE/dx$ response have been carefully parameterized for positively and negatively charged particles using residual variables, keeping into account correlations between residuals.

This has been done extending $dE/dx$ calibration, done on the first 3 fb$^{-1}$, to all data sample. We obtained a separation power for pions and kaons with momentum greater than 2 GeV/$c$ above 1.4$\sigma$, which is consistent with previous estimates of this quantity.

In conclusion we demonstrated that $dE/dx$ calibration can be extended up to P38 without any relevant issue. Therefore the calibration can be used on the entire RunII data sample.

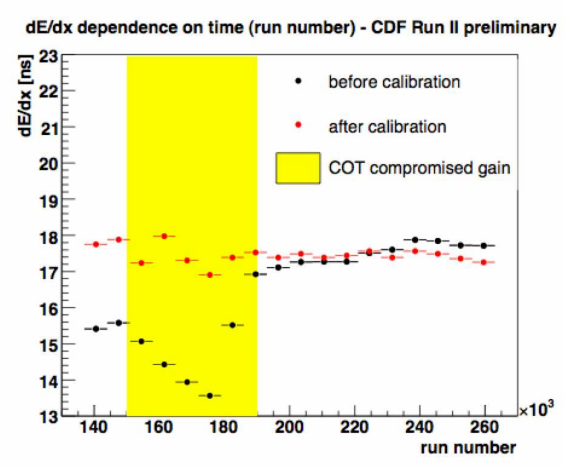


Figure 15: dE/dx in function of run distribution

# A Appendix - Period 0 exclusion

The dataset `xbhdid`, covering a period of run range from 138425 to 186598 (period 0) is the first period produced. For this reasons, it contains some differences with respect to the other periods. One difference, that is substantial for the dE/dx analyses, resides in the dEdx in function of run distribution.It is well known that for Period 0 the performance of the COT in P0 was compromised. The effect on the dE/dx is difficult to calibrate in the first period, as you can see from the plot XXX, from cdfnote 9592. Another difference, that is important for the dE/dx analyses, is the instantaneous luminosity value returned by the BottomMods package. For example, for the $\Lambda \to p\pi^-$ sample described in subsection 2.2, in the first period the fraction of events with instantaneous luminosity value equal to 0 is about 60% of the total, while for the whole datasets the fraction is about 5%, as you can see from fig. 16. The correspondent values decreases for the $D^0 \to K^-\pi^+$ sample (6% in the period 0, 0.5% for the whole periods). This suggests a problem in the way BottomMods access to the database information. Therefore the events coming from the period 0 have an incorrect dE/dx calibration. This wrong calibration could bias the results of this work. For these reasons we decided to exclude the period 0 to produce the universal curves, losing in statistics but gaining in accuracy.

# B Appendix - Comparison between UC parameterizations

The old parameterizations for kaons and pions from `DeDx2008_funcs.C` is overlaid (red line) in Figure 17, while the parameterization from `DeDx2011_funcs.C` is overlaid (black line) in Figure 18.

The old parameterizations for the protons and soft pions from `DeDx2011_funcs.C` is overlaid (black line) in Figure 19.

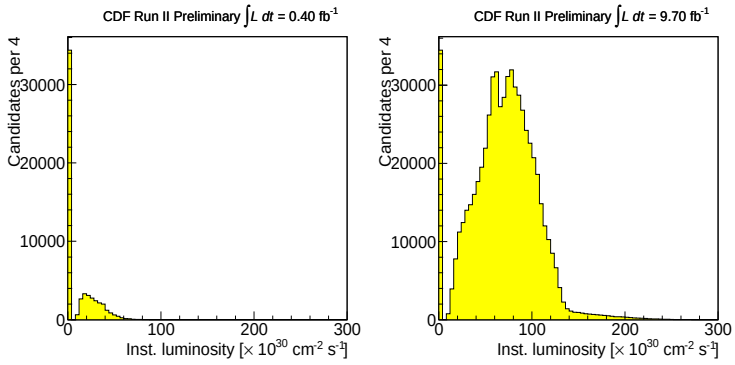


Figure 16: Instantaneous luminosity for $\Lambda \to p\pi^-$ decays. From P0 to P38 on the right, only P0 on the left.

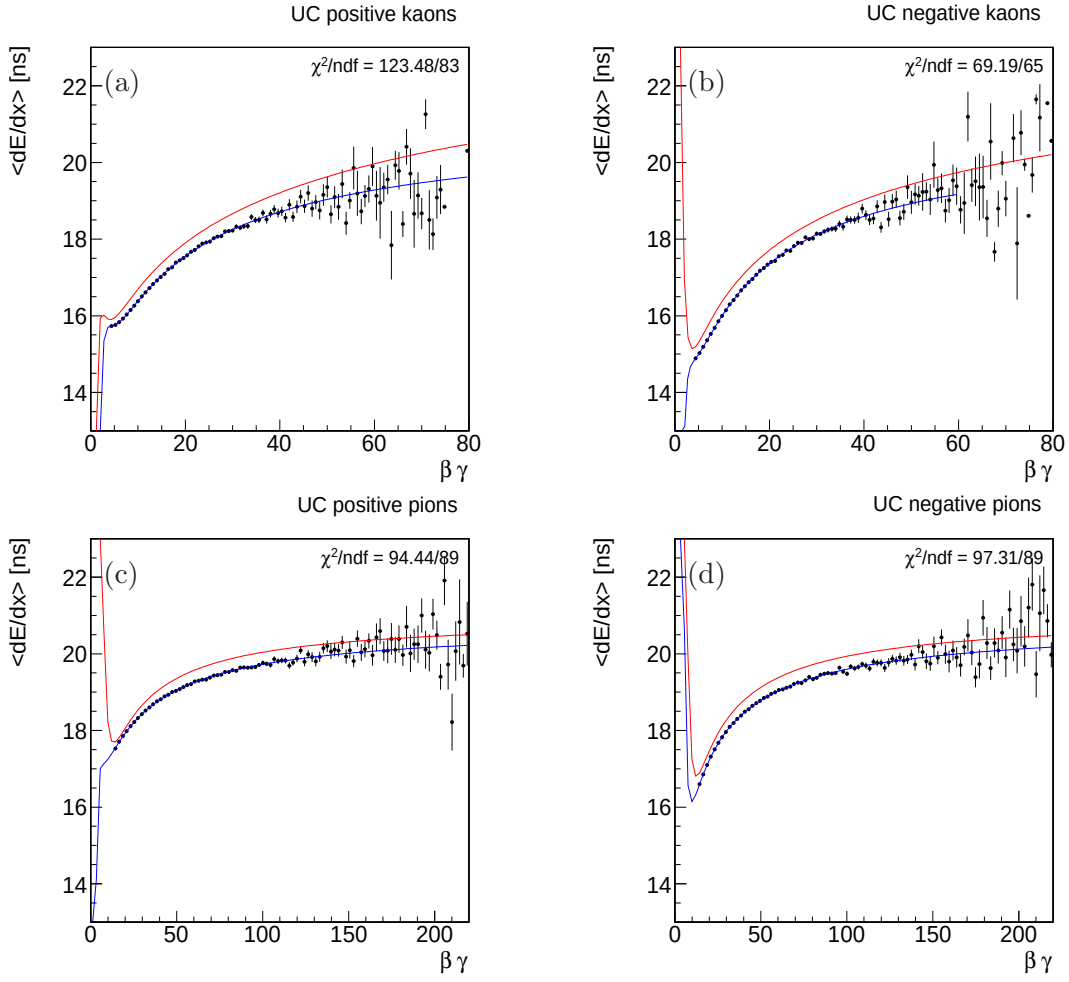


Figure 17: Parameterization (blue) of the Universal Curves for charged pions and kaons from $D^0 \to K^-\pi^+$ decays. Old parameterization from `DeDx2008_funcs.C` (red).

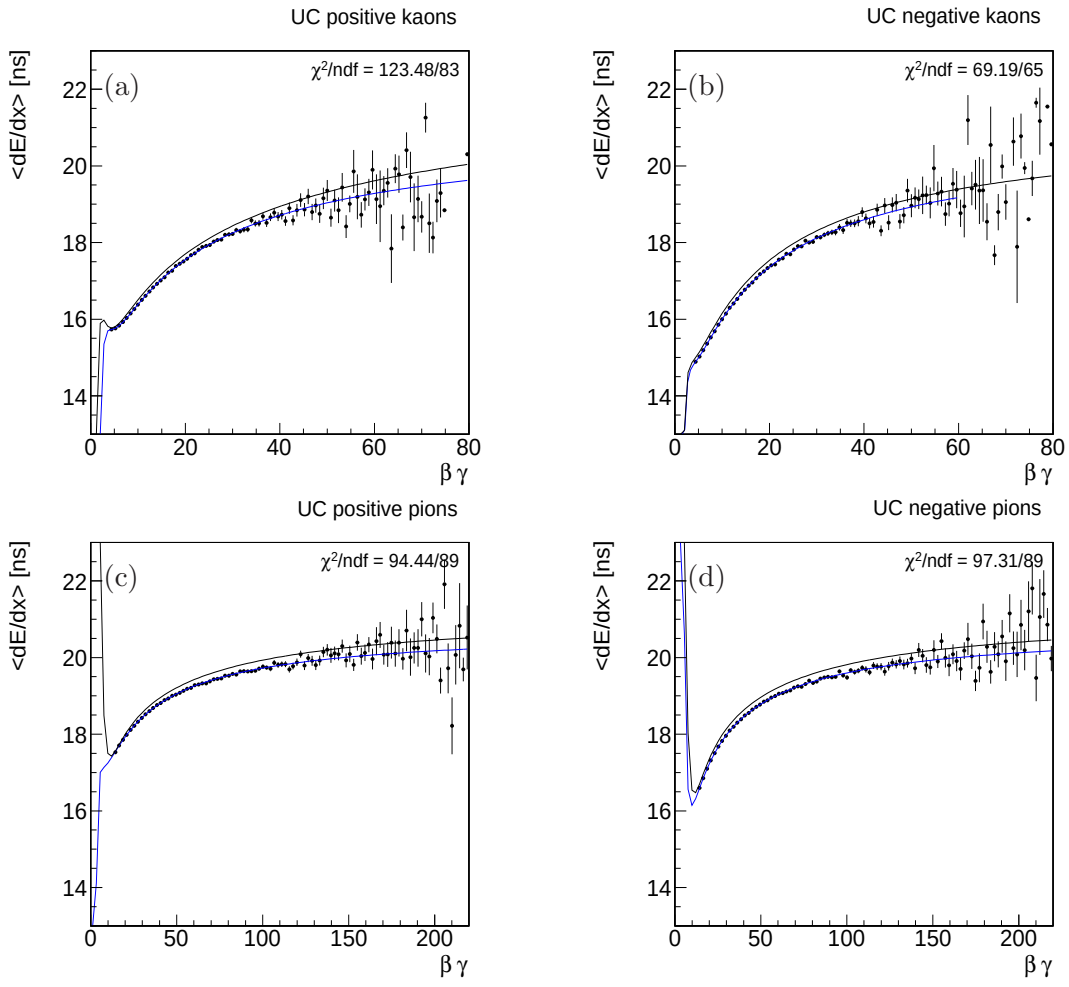


Figure 18: Parameterization (blue) of the Universal Curves for charged pions and kaons from $D^0 \to K^-\pi^+$ decays. Old parameterization from `DeDx2011_funcs.C` (black).

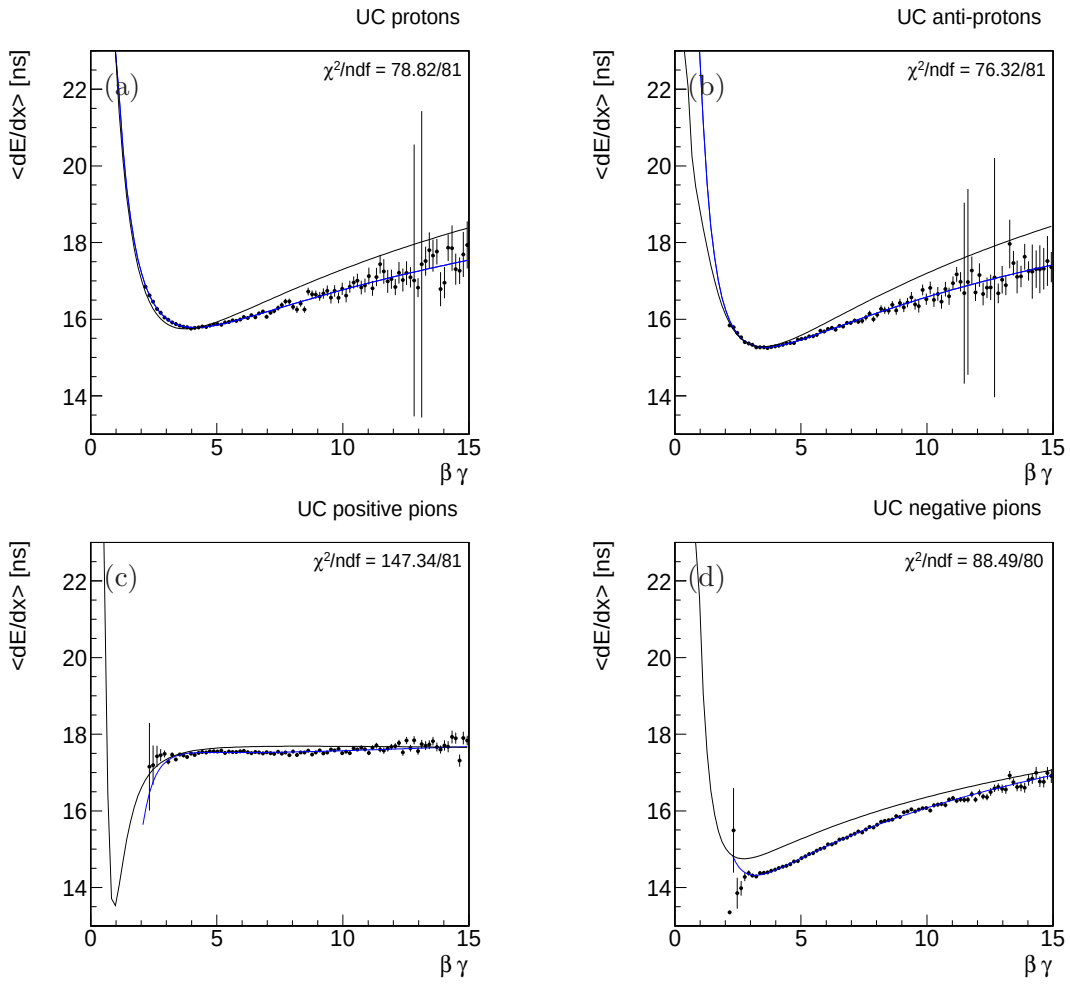


Figure 19: Parameterization (blue) of the Universal Curves for charged pions and protons from $\Lambda \to p\pi^-$ decays. Old parameterization from `DeDx2011_funcs.C` (black).

# C Appendix - Kaons, pions and protons residual with residuals

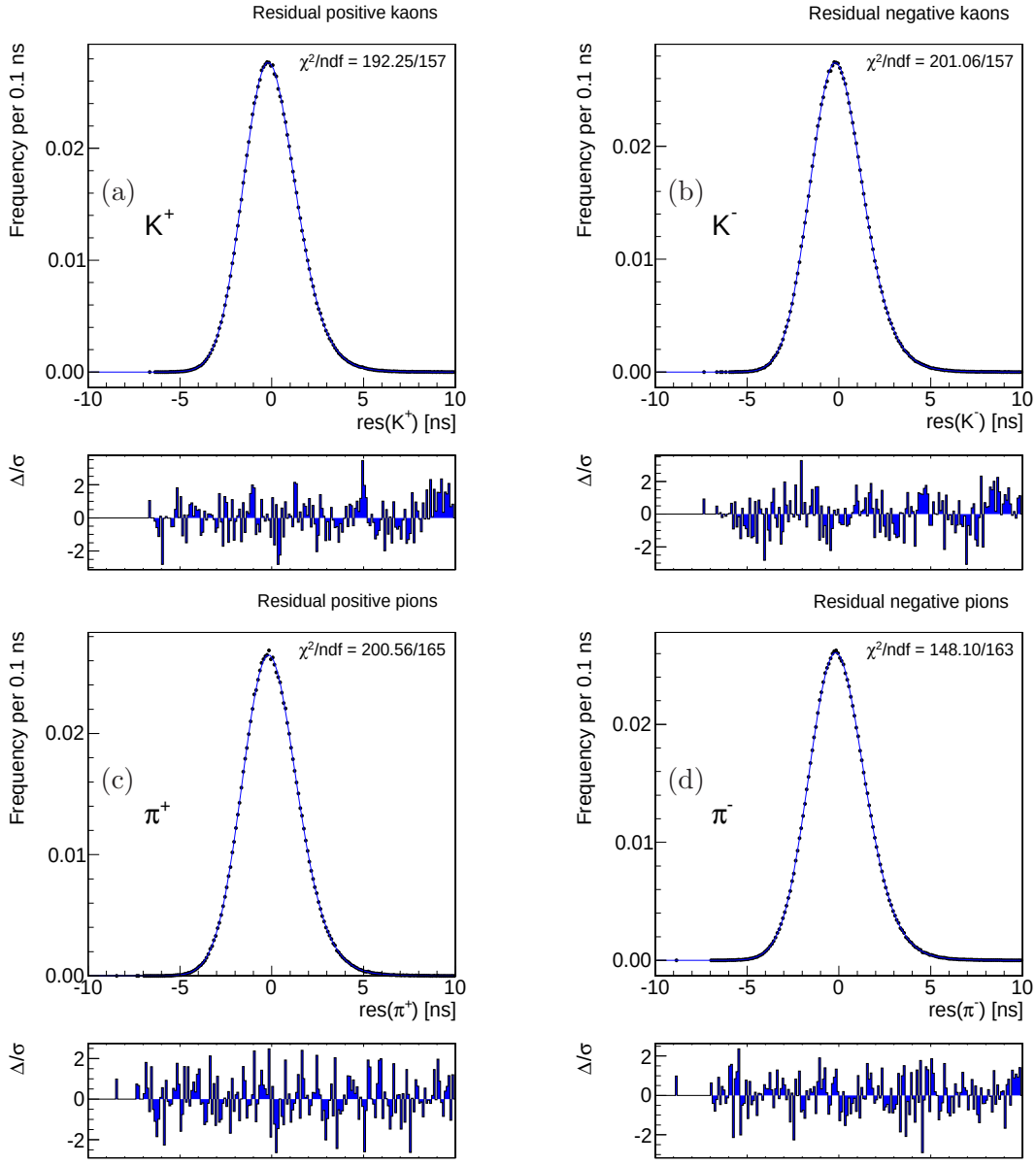


Figure 20: Distribution of observed $dE/dx$ residual ($\wp(\delta^{\text{obs}}) = \wp(\delta + c) = \wp(\delta) * \wp(c)$), for kaons (with kaon mass hypothesis) (a,b), for pions (with pion mass hypothesis) (c,d) The results of the fit to the functions in eq. (16) and eq. (17) are overlaid (blue, solid line).

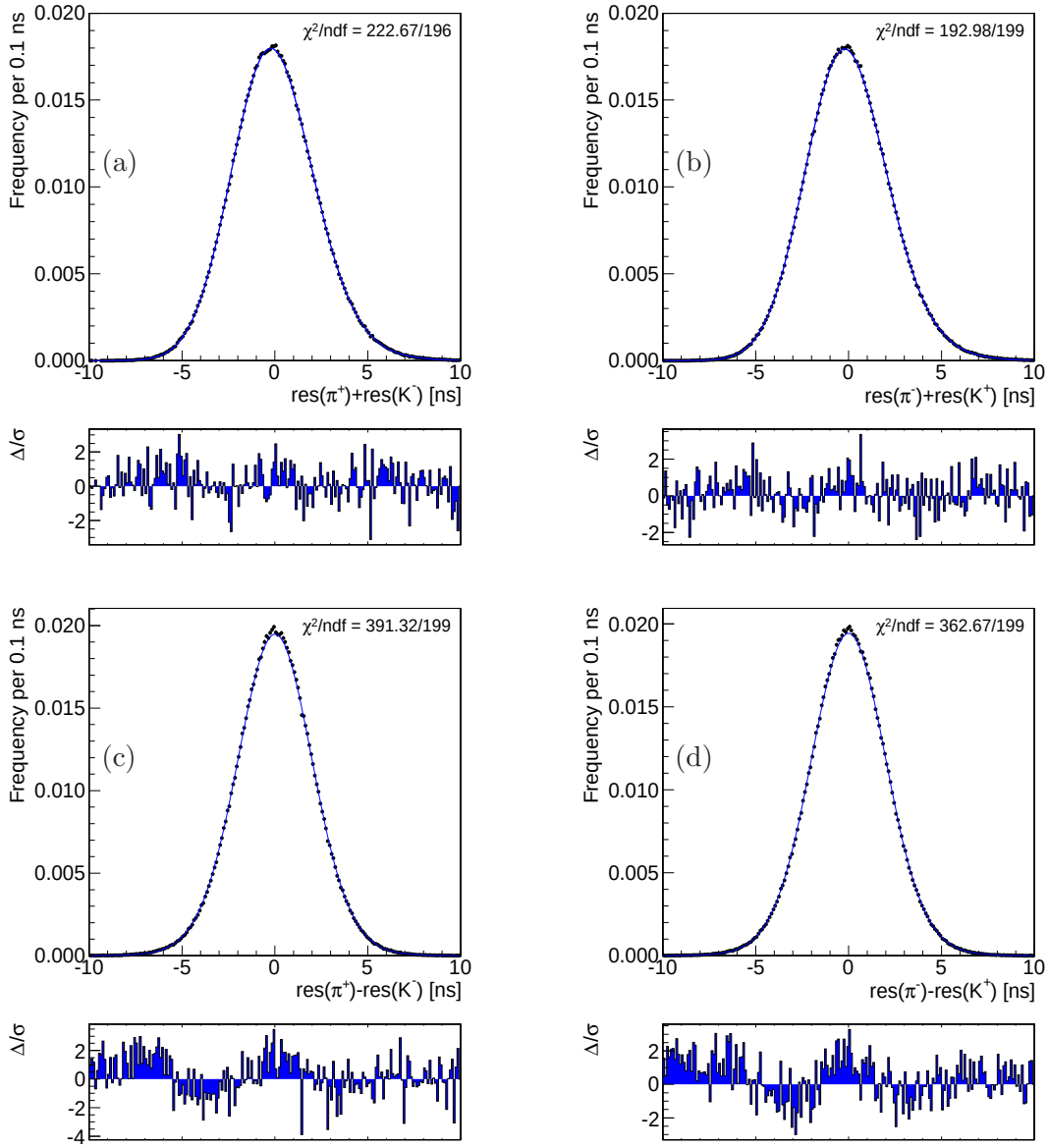


Figure 21: Distribution of the sum (a,b) and the difference (b,d) of the residuals for a kaon (in kaon hypothesis) and a pion (in pion hypothesis) from $D^0 \to K^-\pi^+$ decays. The results of the fit to the functions in eq. (18) and eq. (19) are overlaid (blue, solid line).

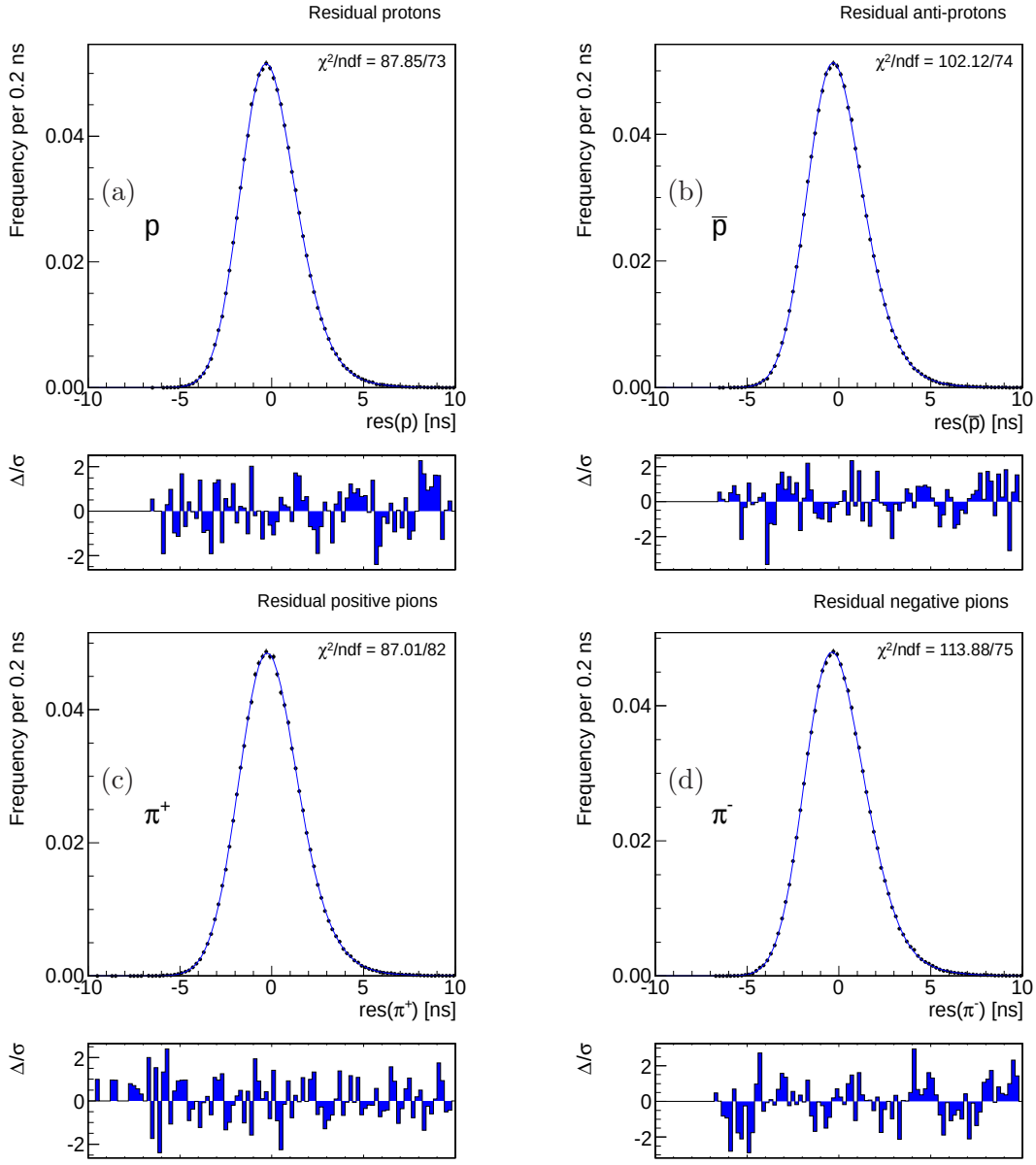


Figure 22: Distribution of observed $dE/dx$ residual ($\wp(\delta^{\rm obs}) = \wp(\delta + c) = \wp(\delta) * \wp(c)$), for protons (with protons mass hypothesis) (a,b), for pions (with pion mass hypothesis) (c,d) The results of the fit to the functions in eq. (16) and eq. (17), where $K \to p$, are overlaid (blue, solid line).

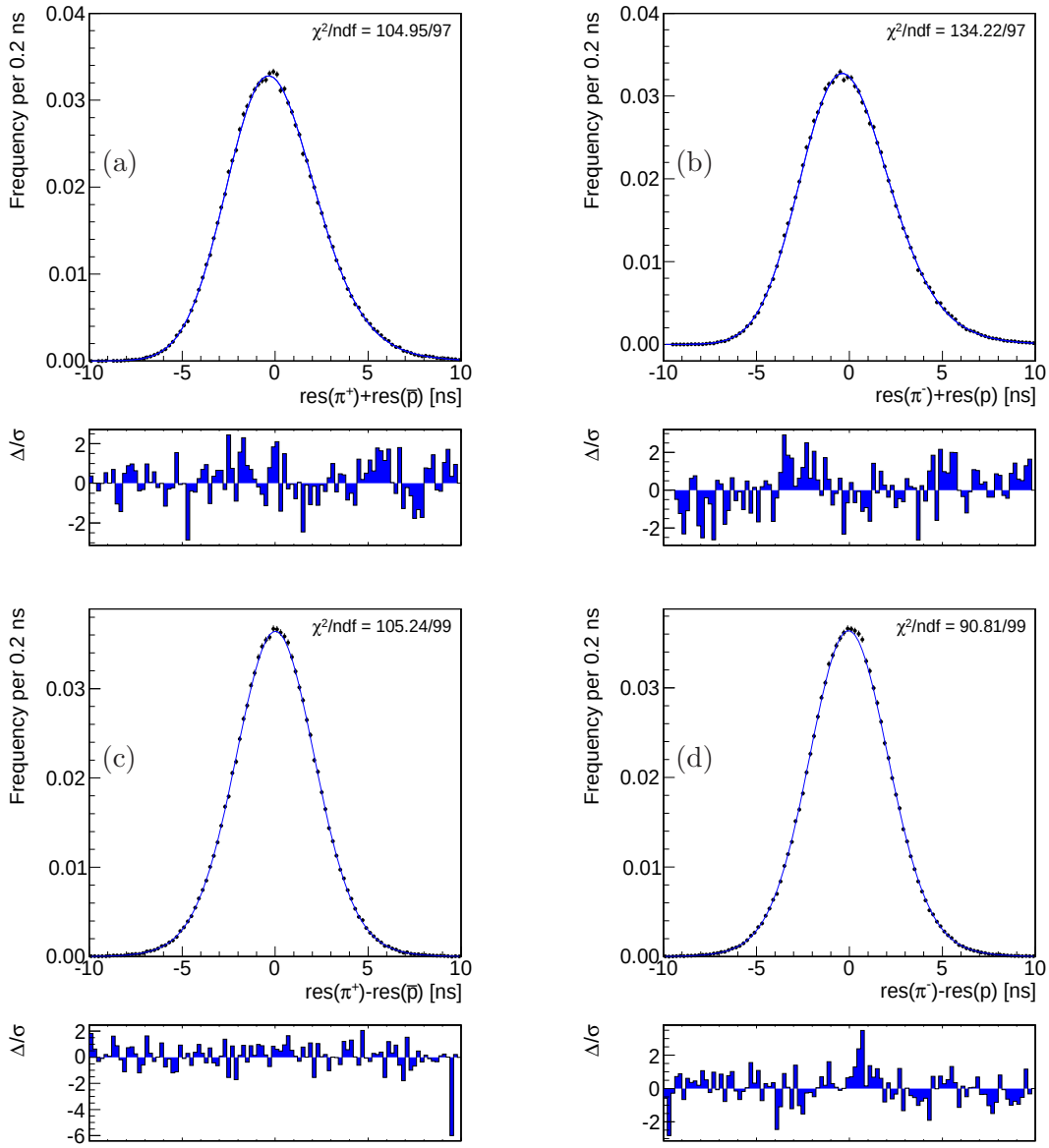


Figure 23: Distribution of the sum (a,b) and the difference (c,d) of residuals for a proton (in proton hypothesis) and a pion (in pion hypothesis) from $\Lambda \to p\pi^-$ decays. The results of the fit to the functions in eq. (18) and eq. (19), where $K \to p$, are overlaid (blue, solid line).

## References


[1] S.-S. 'Eiko' Yu et al., *COT dE/dx Measurement and Corrections*, CDF Internal Note 6361 (2004), unpublished.

[2] F. Azfar, L. Oakes, and D. Tonelli, *Extended and improved dE/dx calibration for 3fb$^{-1}$ analyses*, CDF Internal Note 9592 (2008), unpublished.

[3] A. Di Canto, M. J. Morello, G. Punzi, L. Ristori, and D. Tonelli, *Measurement of Time-integrated CP Asymmetry in $D^0 \to \pi^+\pi^-$ Decays*, CDF Internal Note 10213 (2010), unpublished.

[4] A. Di Canto, M. J. Morello, G. Punzi, L. Ristori, and D. Tonelli, *Measurement of Time-integrated CP Asymmetry in $D^0 \to K^+K^-$ Decays*, CDF Internal Note 10365 (2011), unpublished.

[5] C. Amsler et al. (Particle Data Group), *The Review of Particle Physics*, Phys. Lett. **B667**, 1 (2008).

[6] M. J. Morello, G. Punzi, and F. Ruffini, *Branching Ratios and CP asymmetries in $B^0_{(s)} \to h^+h^{'-}$ decays from 6 fb$^{-1}$*, CDF Internal Note 10443 (2011), unpublished.

[7] M. J. Morello, G. Punzi, and F. Ruffini, *Branching Ratios and CP asymmetries in $B^0_{(s)} \to h^+h^{'-}$ decays from 9 fb$^{-1}$*, in preparation

[8] F. Lazzari, M. J. Morello, G. Punzi, F. Ruffini, and ,,Detector-induced charge asymmetry in $\Lambda \to p\pi^-$ CDF Internal Note 10717 (2011), unpublished.

[9] M.J. Morello, Ph.D. Thesis, Scuola Normale Superiore, Pisa, Fermilab Report No. FERMILAB-THESIS-2007-57 (2007).

[10] M. Campanelli et al., *TOF performance studies with $\Lambda^0$ and $K^0_s$ decays*, CDF Internal Note 6757 (2004), unpublished.

[11] H. A. Bethe, *Theory of passage of fast corpuscular rays through matter*, Annalen Phys. **5**, 325 (1930), in German and *Scattering of electrons*, Z. Phys. **76**, 293 (1932); F. Bloch, *Stopping power of atoms with several electrons*, Z. Phys. **81**, 363 (1933).

[12] G. Punzi, *Useful formulas on statistical separation of classes of events*, [physics/0611219].

[13] M. J. Morello, G. Punzi, and F. Ruffini, *dE/dx for pions, kaons and protons for 6 fb$^{-1}$ analyses*, CDF Internal Note 10442 (2011), unpublished.

[14] S. D'Auria et al., *Track-based calibration of the COT specific ionization*, CDF Internal Note 6932 (2004), unpublished.

[15] M.A. Ciocci, G. Punzi, and P. Squillacioti, *Update of Combined PID in 6.1.4*, CDF Internal Note 8478 (2006), unpublished;
G. Punzi and P. Squillacioti, *Update of Combined PID in 5.3.4*, CDF Internal Note 7866 (2005), unpublished;
R.Carosi et al., *Particle Identification by combining TOF and dEdx information*, CDF Internal Note 7488 (2005), unpublished.

[16] D. Tonelli, *First observation of the $B^0_s \to K^+K^-$ decay mode, and measurement of the $B^0$ and $B^0_s$ mesons decay-rates into two-body charmless final states at CDF.*, Ph. D. thesis, Scuola Normale Superiore, Pisa, FERMILAB-THESIS-2006-23 (2006).

[17] P. Squillacioti, *Measurement of the branching fraction ratio $\mathcal{B}(B^+ \to \overline{D}^0K^+)/\mathcal{B}(B^+ \to \overline{D}^0\pi^+)$ with the CDF II detector.*, Ph. D. thesis, University of Siena, Siena, FERMILAB-THESIS-2006-27 (2006).